

A review paper about experimental investigations on failure behaviour of non-persistent joint

Alireza Bagher Shemirani¹, Hadi Haeri^{*2}, Vahab Sarfarazi^{**3}
and Ahmadreza Hedayat⁴

¹Department of Civil Engineering, Sadra Institute of Higher Education, Tehran, Iran

²Young Researchers and Elite Club, Bafgh Branch, Islamic Azad University, Bafgh, Iran

³Department of Mining Engineering, Hamedan University of Technology, Hamedan, Iran

⁴Department of Civil and Environmental Engineering, Colorado School of Mines,
Golden, Colorado 80401, U.S.A.

(Received September 18, 2016 Revised February 26, 2017, Accepted March 21, 2017)

Abstract. There are only few cases where cause and location of failure of a rock structure are limited to a single discontinuity. Usually several discontinuities of limited size interact and eventually form a combined shear plane where failure takes place. So, besides the discontinuities, the regions between adjacent discontinuities, which consist of strong rock and are called material or rock bridges, are of utmost importance for the shear strength of the compound failure plane. Shear behaviour of persistent and non-persistent joint are different from each other. Shear strength of rock mass containing non-persistent joints is highly affected by mechanical behavior and geometrical configuration of non-persistent joints located in a rock mass. Therefore investigation is essential to study the fundamental failures occurring in a rock bridge, for assessing anticipated and actual performances of the structures built on or in rock masses. The purpose of this review paper is to present techniques, progresses and the likely future development directions in experimental testing of non-persistent joint failure behaviour. Experimental results showed that the presence of rock bridges in not fully persistent natural discontinuity sets is a significant factor affecting the stability of rock structures. Compared with intact rocks, jointed rock masses are usually weaker, more deformable and highly anisotropic, depending upon the mechanical properties of each joint and the explicit joint positions. The joint spacing, joint persistency, number of rock joint, angle of rock joint, length of rock bridge, angle of rock bridge, normal load, scale effect and material mixture have important effect on the failure mechanism of a rock bridge.

Keywords: non-persistent joint; rock bridge; shear mechanism; experimental test

1. Introduction

Lengths of the fractures in natural rocks can vary from tens of kilometres down to tens of microns. In addition, the joints in rocks are normally discontinuous in nature with limited lengths. There are only few cases where the cause and the location of failure in rock structure limited to a single discontinuity. Usually, several discontinuities of limited size interact and eventually form a

*Corresponding author, Assistant Professor, E-mail: h.haeri@bafgh-iau.ac.ir or haerihadi@gmail.com

**Corresponding author, Assistant Professor, E-mail: vahab.sarfarazi@gmail.com or Sarfarazi@hut.ac.ir

combined shear plane where the failure takes place (Committee on Fracture Characterization and Fluid Flow 1996). So, besides the discontinuities themselves, regions between adjacent discontinuities consisting strong rock which called the rock bridges are of utmost importance for the shear strength of compound failure plane (Jaeger 1971, Einstein *et al.* 1983) (Fig. 1(a)). From the practical point of view and to a certain extent, in nearly all rock engineering projects, constructions of structures in or on rock masses contain both; fractures and rock bridges. The crack coalescence in a rock bridge is usually responsible for the failure of many rock structures. Also, higher strength of rock mass is mainly induced by the presence and the arrangement of rock bridges (Stimpson 1978, Jennings 1970, Zhao 1995, Horii *et al.* 1986). One claims to be on the safe side since the rock bridges are thought to produce a strength reserve, as they have to be broken first before failure can take place along the newly separated plane (Stimpson 1978). In some approaches, the rock bridges are taken to be responsible for increasing additional cohesive strength (Einstein *et al.* 1983, Stimpson 1978, Jennings 1970). From other point of views, the collapse of underground structures can be regarded as either; the movement of fractured block in fully persistent jointed rock masses, or propagation and coalescence of non-persistent joints around excavation surface. Therefore, the mechanism of crack coalescence in the rock bridge area between pre-existing joints remains one of the most fundamental theoretical problems in rock mechanics to be solved. A comprehensive study on the shear failure behaviour of jointed rock can provide a good understanding of local and general rock instabilities, leading to improved designs for the rock engineering projects. In the following sections, experimental and numerical studies will be described.

2. Experimental analyses

2.1 A common crack pattern found in rocks and rock-model materials under compressive loading

Crack initiation and propagation have been the subjects of intensive investigations in rock mechanics, both theoretically and experimentally. First theoretical study on growth of the pre-existing two-dimensional cracks was given by Griffith (1921, 1924). Irwin (1957) further introduced the concept of critical energy release rate and the crack tip stress intensity factor (K). With respect to the field of rock mechanics, a number of experimental studies have been carried out to investigate the crack initiation, propagation and interaction (Hoek *et al.* 1965, Pang *et al.* 1972, Hallbaue *et al.* 1973, Tapponn *et al.* 1976, Olsson *et al.* 1976, Kranz 1983, Batzle *et al.* 1980, Kim *et al.* 2012, Kumar and Barai 2012, Lin *et al.* 2014, Kim and Taha 2014, Haeri *et al.* 2014a, 2014b, Ning *et al.* 2015, Weihua *et al.* 2015, Yang 2015, Gerges *et al.* 2015, Panaghi *et al.* 2015, Chen *et al.* 2015, Haeri 2015a, b, Haeri *et al.* 2015a, b, c, d, Haeri and Sarfarazi 2016a, b, Sardemir 2016). For a comprehensive literature review on micro-crack studies, it refers to Kranz (1983). Meanwhile, many mathematical models were developed to explain and predict the processes of crack growth, interaction and rock failure (Dey *et al.* 1981, Steif 1984, Horii *et al.* 1985, Ashby *et al.* 1986, Sammis *et al.* 1986, Kemeny *et al.* 1987, Kemeny 1991). For discussing on how these shear crack models can be applied to real rocks, it refers to the comparative study by Fredrich *et al.* (1990). A number of researches were described their studies on crack propagation on different materials in uniaxial compression forms (Hoek and Bieniawski 1984, Jiefan *et al.* 1990). A common crack pattern found in rocks and rock-model materials under compressive loading was also summarized by Bobet (2000) as follows (see Fig. 1): 1. Wing cracks start at the

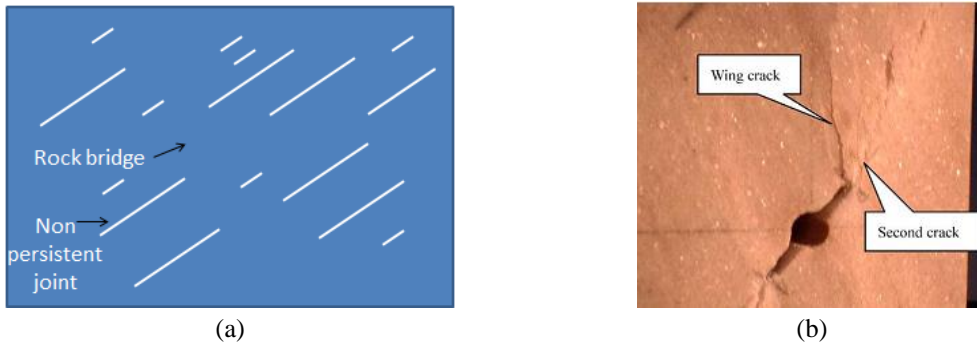


Fig. 1 (a) The schematic view of non-persistent joint and rock bridge and (b) A common crack pattern found in rocks and rock-model materials, Bobet (2000)

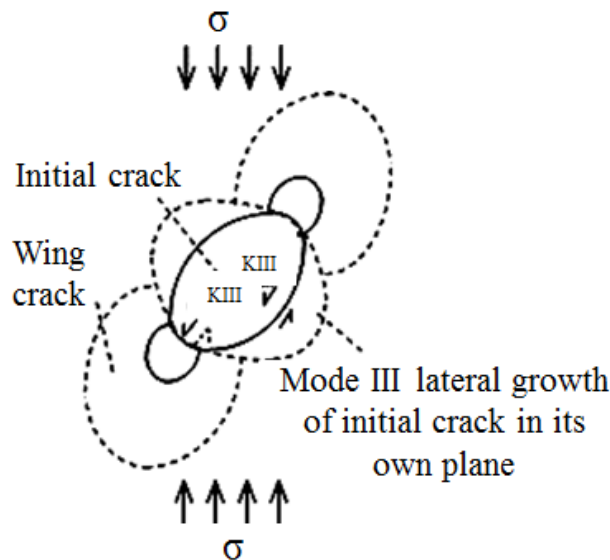


Fig. 2 A sketch of the mechanism of 3-D crack growth as hypothesised by Dyskin and Salganik (2003)

tips of the fractures and propagate in a curvilinear path as load increases. Wing cracks as the tensile type grow in stable manner, since an increase in loading is necessary to lengthen the cracks. Wing cracks tend to align with the direction of the most compressive stress. 2. Secondary cracks are generally described as shear cracks or shear zones. They initiate from the tips of the fractures and there two directions are possible: (1) coplanar or nearly coplanar to the fractures; (2) with an inclination similar to wing cracks but in opposite direction.

2.2 Crack growth in PMMA plate under compressive loading

Dyskin *et al.* (2003) have investigated the influence of shape and locations of initial 3-D cracks on their growth in uniaxial compression (Fig. 2).

Tests undertaken on different materials such as transparent casting resin, cement and mortar, as well as tests on PMMA and bore-silicate glass samples (19, 20), using different techniques for

producing internal initial cracks of different shapes and sizes demonstrate that 3-D crack growth in compression qualitatively differs from the 2-D case. Unlike 2-D cracking, there are intrinsic limits on 3-D growth of wing cracks produced by a single pre-existing crack (Figs. 3-4). This limitation is related to the wing wrapping and, possibly, to the inability of the initial crack to extend itself in a lateral direction; a pre-requisite for maintaining a mechanism of wing growth similar to that observed in 2-D tests. Although it is conceivable that the structural elements of heterogeneous materials can enable the lateral growth of initial cracks, the presence of multitudes of cracks provides a self-sufficient mechanism of failure. Even if the growth of single discrete cracks is restricted, the effect of interaction can produce new cracks that substantially propagate towards the loading direction. In heterogeneous materials many new cracks are produced during loading, as evident from acoustic emission studies. Therefore, it can be assumed that this concentration of cracks will ultimately produce the described mechanism of large fracture formation.

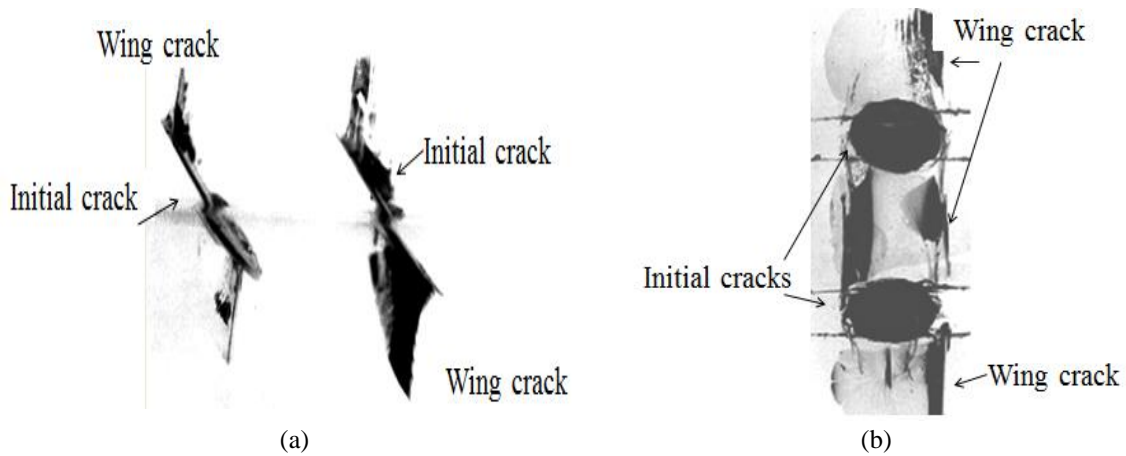


Fig. 3 (a) Fragment of a resin sample with horizontally aligned parallel cracks and (b) Fragment of a resin sample with vertically aligned parallel cracks (horizontal lines are threads holding the inclusions)

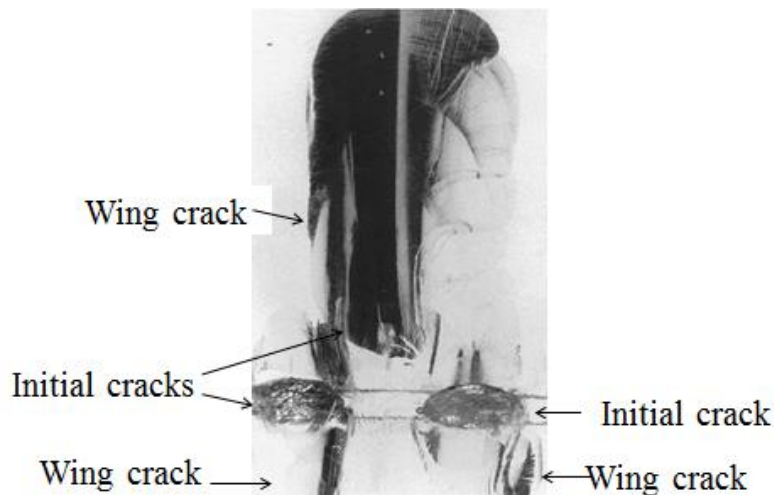


Fig. 4 Fragment of a resin sample with horizontally aligned coplanar cracks

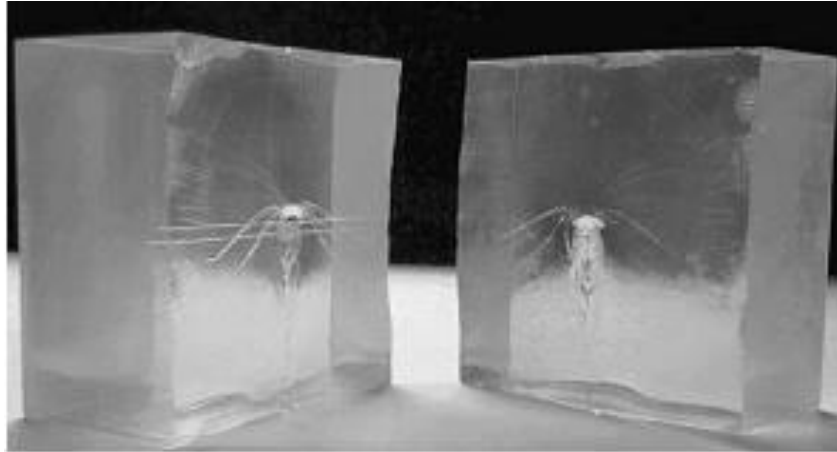


Fig. 5 Helical wings growing from the initial crack

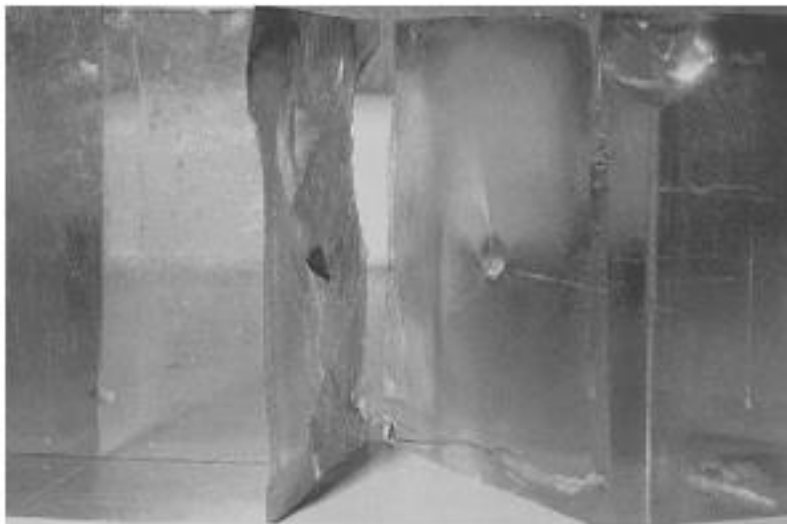


Fig. 6 Extensive wing growth in resin causing splitting under biaxial compression

The conducted tests under true biaxial compression showed that all samples failed by splitting parallel to the free surface. The wings emerging from the initial inclined crack in resin grew extensively towards both loading axes. One wing, the lower branch, extended in a helical direction, vertically towards the sample boundary. This behaviour was different from that observed under uniaxial compression where the growth was restrained by the wrapping (curling) mechanism of the wings.

2.3 3D crack growth from two pre-existing flaws in rock-like material under compressive loading

Tang *et al.* (2015) have investigated Mechanical Behavior of 3D Crack Growth in Transparent Rock-Like Material Containing Pre-existing Flaws under Compression (Fig. 7).

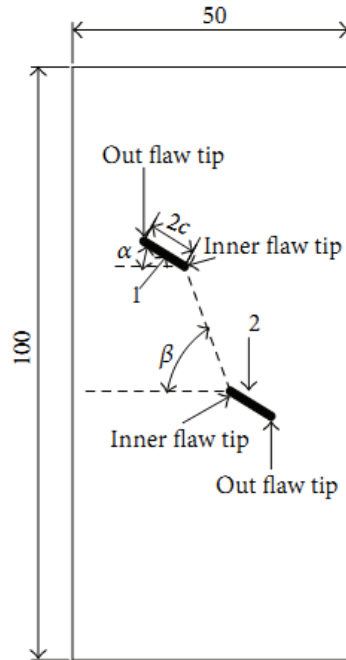


Fig. 7 A specimen containing two pre-existing flaws: the inclinations are α , the rock bridge angle is β and the length of the pre-existing flaw is $2c$

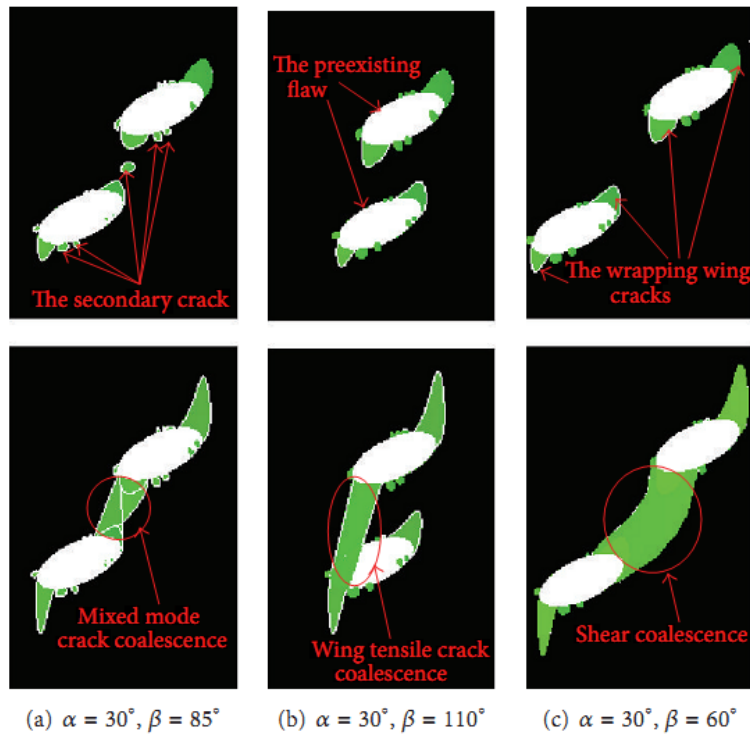


Fig. 8 Three different patterns of 3D crack coalescence are observed in the tests

The results shows that coalescence in 3D flaws with different rock bridge angles can be identified as the shear mode, the mixed mode (tensile mode and shear mode), and wing tensile mode (Fig. 8).

When the inclination angle $\alpha=30^\circ$ and frictional coefficient $\mu=0.57$, the coalescence mode is dominated by different rock bridge angles. When $\beta=60^\circ$, shear mode coalescence occurs; when $\beta=85^\circ$, mixed mode coalescence occurs; when $\beta = 110^\circ$, wing tensile mode coalescence occurs. Nevertheless, more 3D experimental and theoretical studies need to be carried out.

Ingrafea and Heuze (1980) observed similar crack pattern in uniaxial compression tests on limestone and grano diorite specimens with single inclined flaws. Petit and Barquins (1988) studied crack propagation in sandstone from a single flaw subjected to uniaxial compression; tensile cracks, or “Branch Fractures”, and a “Shear Zone” were observed at the tips of the flaw. Chen *et al.* (1992) conducted uniaxial experiments on marble; first, tensile cracks appeared near and at the tip of the flaw. As the load was increased, an “X” shape band appeared at and extended from the tips of the flaw approaching to the specimen boundary.

A number of investigators have reported cracks with similar characteristics in the specimens containing single inclined flaw (Einstein *et al.* 1993, Pang *et al.* 1972, Hallbauer 1973, Tapponnier *et al.* 1976, Olsson *et al.* 1976, Kranz 1979, Batzle *et al.* 1980, Dey *et al.* 1981, Germanovich 1996, Steif 1984, Sagong *et al.* 2000, Bieniawski 1967, Jamil 1999, Alzoubi 2001, Bobet 1997, Bobet *et al.* 1998, Celestino *et al.* 2001, Huang *et al.* 1999, Li *et al.* 2003, Papadopoulos *et al.* 1983, Shah 1999a, Shah 1999b, Shang 1999, Shen 1993, Shen *et al.* 1995, Tang *et al.* 1998, Takeuchi 1991, Wong *et al.* 1998, Deng *et al.* 1984, Zhu *et al.* 1998). Reyes (1991), Shah (1999a,b), Shen (1993, 1995), Bobet (1997), Bobet and Einstein (1998), Zhu *et al.* (1998), Wong and Chau (1998) and Wong *et al.* (1997) have investigated crack propagation and coalescence on rock-like materials specimens containing two inclined flaws which both were either open or closed. Besides model materials, real rock samples are also employed to study the rock materials with fractures.

Examples include the work of Huang *et al.* (1999) and Celestino *et al.* (2001) on marble and Shang *et al.* (1999) on granite and marble. They found that wing cracks and secondary cracks (initiating after the wing cracks) may occur and eventually lead to coalescence under uniaxial compression. To incorporate the effect of crack surface friction, Shen *et al.* (1993) conducted a series of uniaxial compressive tests on gypsum specimens containing both, open and closed fractures. It was found that the initial geometrical setting of parallel flaws controls the mechanism of crack coalescence. The observed patterns of crack coalescence were similar to those reported in the study by Wong and Chau (1998). Failure of flawed solids may occur in tensile and/or shear modes, depending on geometrical relation between the two pre-existing flaws.

2.4 Crack growth from two pre-existing frictional flaws in rock-like material under compressive loading

Based upon the experimental work by Wong and Chau (1998) and Shen *et al.* (1995), Wong and Chau (1997) reconsidered the problems of crack coalescence and the strength between the two flaws by using a rock-like material (made of barite, sand, plaster and water) under uniaxial compression (Fig. 9). Three main factors were changed to investigate the failure patterns: the flaw angle ‘ α ’ (inclination of the flaw), the bridge angle ‘ β ’ (angle between two flaws) and the frictional coefficient ‘ μ ’ of flaw surface (Fig. 9(b)), under the conditions of a fixed flaw length ‘ $2c$ ’ and a fixed distance between the flaws ‘ $2b$ ’.

In general, three main modes of crack coalescence were observed as shown in Fig. 10. They are

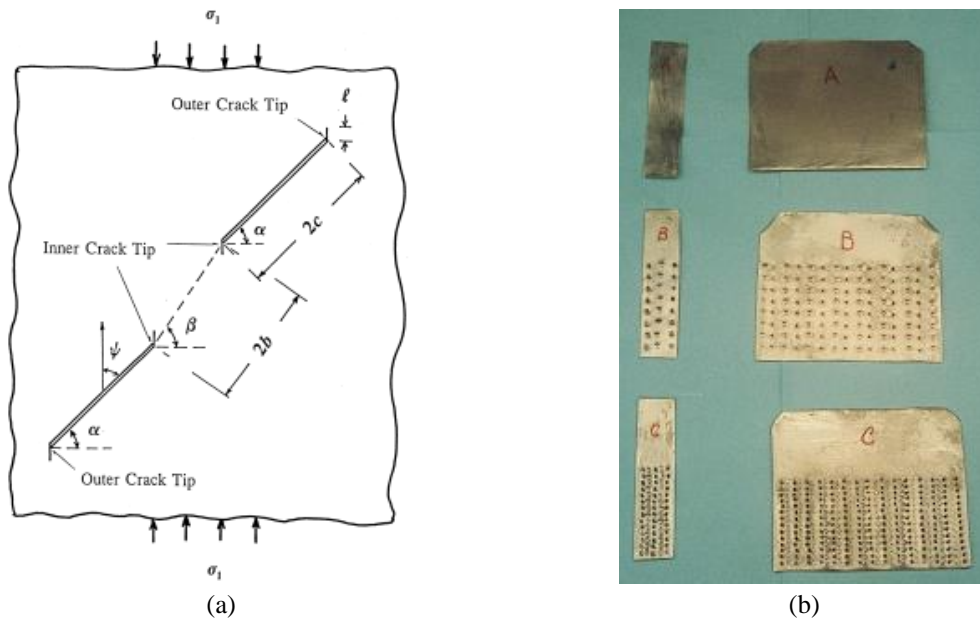


Fig. 9 A solid containing two neighbouring sliding cracks of length $2c$ with wing cracks of length $2b$ subjected to uniaxial compression. the bridge distance between the two pre-existing cracks is $2b$. The crack inclination α and rock bridge angle β are defined together the location of inner and outer crack tips and (b) stainless steel sheets with different roughness used in creating the sliding cracks in the modelling material

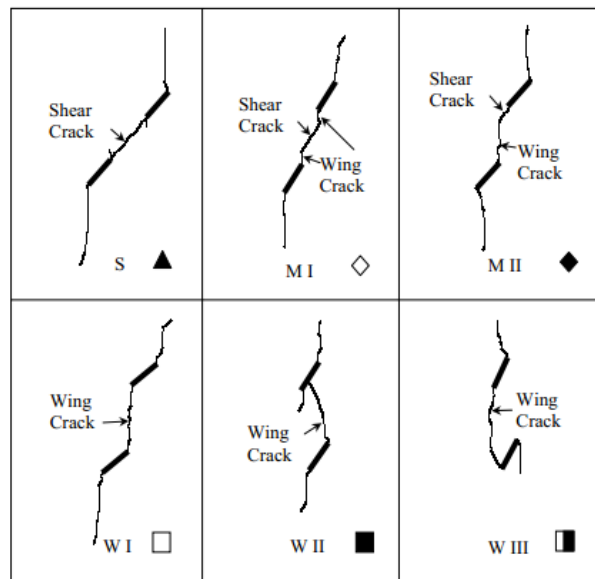


Fig. 10 Three main modes of crack coalescence Wong and Chau (1998)

the wing tensile mode (crack coalescence involving the growth of wing cracks along the direction parallel to the compression), the shear mode (links between two flaws along the direction roughly

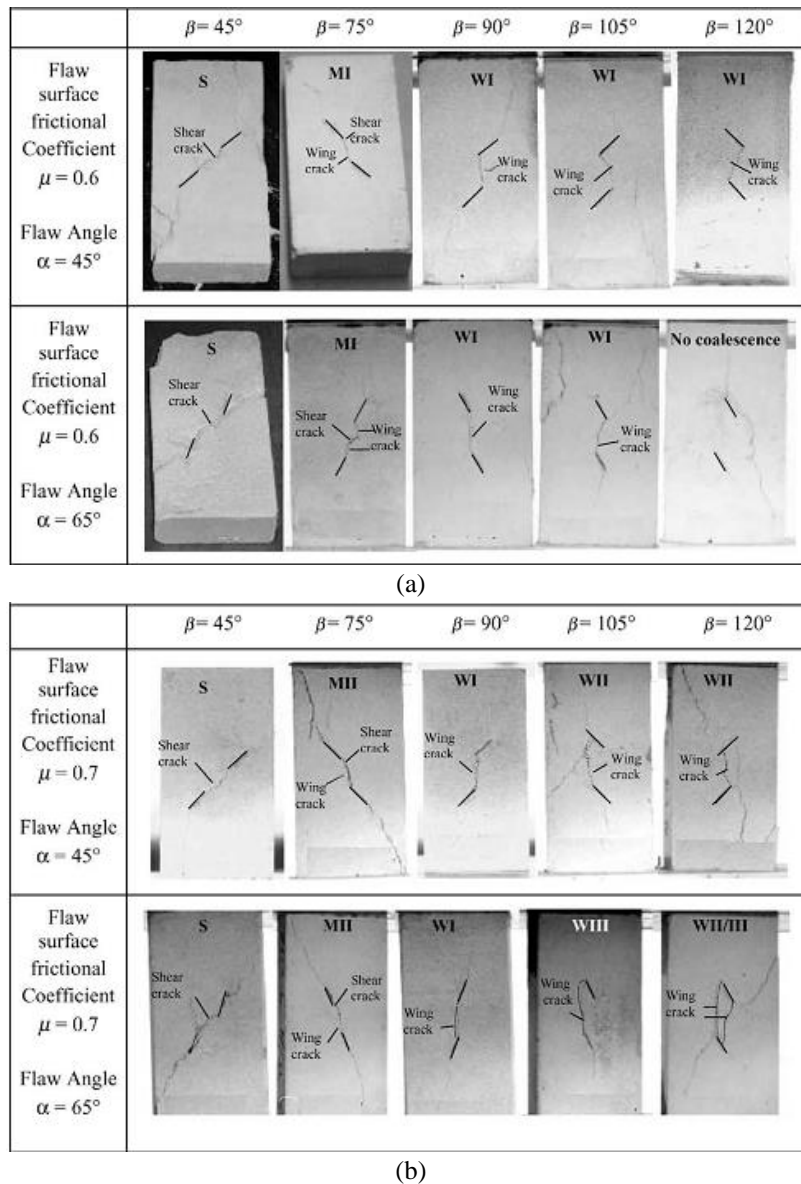


Fig. 11 The mode of crack coalescence for specimens containing two flaws. The angles α represents the bridge angle with (a) $\mu=0.6$ and (b) 0.7

parallel to the flaw), and the mixed mode (shear/tensile). Wong and Chau (1998) proposed a classification of patterns for three different failure modes (tensile, shear and mixed), for different combinations of flaw angle α ; bridge angle β and frictional coefficient μ on flaw surface (Fig. 11). The notations S (shear mode crack coalescence), MI, MII (mixed mode crack coalescence), WI, WII, WIII and WII/III (wing tensile mode crack coalescence) are the same as those proposed in Fig. 6 of Wong and Chau (1997).

Wong (1997), Wong *et al.* (1997, 1998) and Wong and Chau (1998) found that compressive

strength of specimen for the wing crack coalescence is normally lower than that for the shear crack coalescence. Furthermore, Wong and Chau (1998) found that the strength of cracked solids does not show any linear relation with the number of pre-existing flaws (density) once a threshold value of flaw density is exceeded. Also by increasing the friction coefficient the failure surface propagate in different direction. When $\mu=0.6$ the compressive strength is lower than that for the $\mu=0.9$ (Fig. 12).

In those researches, the effect of confining pressure on crack growth properties has eliminated.

Model tests have been conducted to study the effect of structural planes on the deformation characterizes of rocks by Hu *et al.* (2009), and the strength computing method of rock with intermittent joints is proposed. The deformation characterizes of rocks contain structural planes are analyzed by Mao *et al.* (2009).

Hall *et al.* (2006) has investigated the fracture growth in a soft rock consisting imbedded non-persistent joint using acoustic emissions and digital images.

Based on the observations made, for tuff Neapolitan fine-grained, failure is highly dependent on the juxtaposition of the flaws. As such, a general description of the fracture development and coalescence in the rock bridge has been identified with three phases similar to that in a classical form. Few precursory warning signals to failure have been identified, even in the AE analysis.

In situ any precursory signals are most likely to be from with AE signatures, in particular their location, frequency character, the ratio of the cumulative hits and the cumulative energy parameter detected with AE sensors local to high risk fracture zones. Such data might allow the assessment of what stage/type of failure is occurring and so the state of coalescence of the fracturing might be inferred. Even though the observations showed that the coalescence mechanisms may lead very rapidly to failure with only a slight prior warning from the AE monitoring, in situ collapses will occur as the result of many such rock-bridge failures and under different stress conditions. Therefore monitoring with AE within the cavities below Naples may allow tracking of rock-bridge failures and assessment of the overall likelihood of block detachment and large failures. In this research, the effect of non-persistent joint on the shear behaviour of rock bridge is ambiguous.

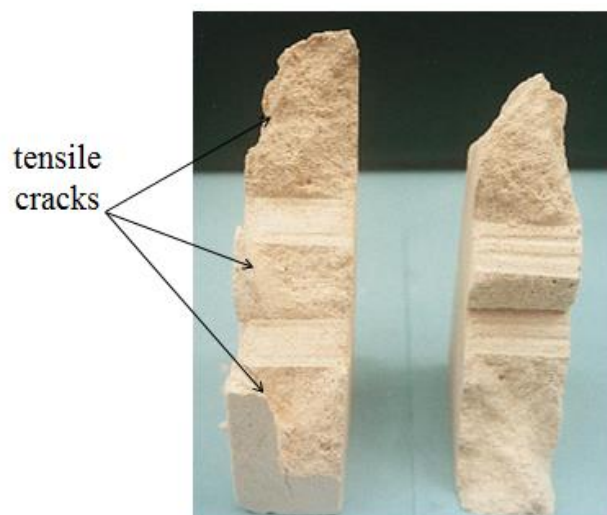


Fig. 12 Showing the final surface roughness of the cracks for $\mu=0.7$ and $\mu=0.9$

Table 1 Classification for three types of crack coalescence

Type	Schematic path of coalescence	Description	Bridge angle	Mode of coalescence
I		Crack coalesce occurred by shear crack	$\beta < 90^\circ$	Shear
II-1		Wing crack initiated from the inner tips of pre-existing crack and coalescence occurred by its propagation	$\beta = 90^\circ$	Tension
II-2		crack and coalescence occurred by tension crack which initiated in the middle of rock bridge during the wing crack propagation	$\beta = 90^\circ$	Tension
II-3		Wing crack initiated from the inner tips of pre-existing crack and coalescence occurred by wing crack in the middle of pre-existing crack	$\beta > 90^\circ$	Tension
II-4		Wing crack initiated from the inner tips of pre-existing crack and coalescence occurred by wing crack in the outer tips of pre-existing crack	$\beta > 90^\circ$	Tension
II-5		crack and coalescence occurred by tension crack which initiated in the middle of rock bridge during the wing crack propagation	$\beta > 90^\circ$	Tension
II		Wing crack initiated from the inner tips of pre-existing crack and coalescence occurred by shear crack which propagated from the wing crack		Shear+ Tension

2.5 Crack growth from two neighbouring pre-existing cracks in rock-like material under uniaxial compression

Park *et al.* (2001) have studied the Crack Coalescence in Rock Bridges under Uniaxial Compression (Fig. 13).

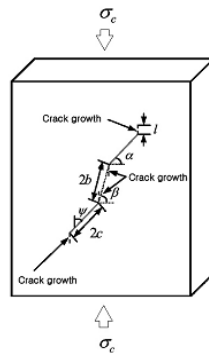


Fig. 13 Model containing two neighbouring pre-existing cracks of length $2c$

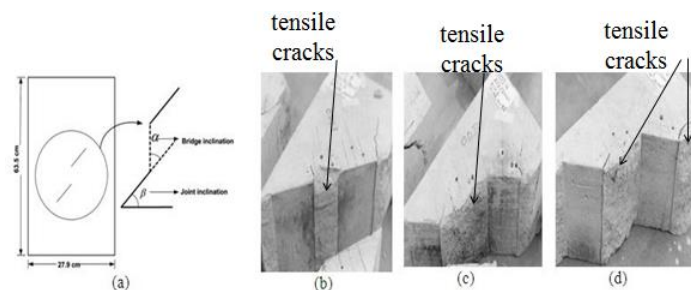


Fig. 14(a) Geometry of specimens and the pre-existing cracks, (b) Upper side of the failure surface $K=0.6$, $\alpha=0^\circ$, $\beta=45^\circ$, (c) $K=0.6$, $a=30^\circ$, $b=45^\circ$ and (d) $K=0.6$, $a=45^\circ$, $b=45^\circ$, Mughieda *et al.* (2004)

The dimension of the specimens was $60 \times 120 \times 25$ mm. Two pre-existing cracks were created in the width of 0.3 mm. The positions and orientations of pre-existing cracks were determined by varying pre-existing crack angle, bridge angle, pre-existing crack length $2c$, and bridge length $2b$. Pre-existing crack angle varied from 30° to 75° with 15° increments and bridge angle was angled at 45° , 60° , 90° , 120° , 135° and 150° to examine the effect of non-overlapping cracks ($\beta < 90^\circ$) and overlapping cracks ($\beta \geq 90^\circ$). Pre-existing crack length and bridge length varied with 10, 15 and 20 mm. The results show that wing crack initiation stress was increased with the increase of pre-existing crack angle. Three types of crack coalescence occurred; Type I was shear cracking, Type II was tensile cracking, which was later divided into five different sub-types, and Type III was a mixture of shear and tensile cracking. Classification by the types of crack coalescence depended on bridge angle. When the bridge length lies between 1.5 and 2 times of crack length, crack coalescence did not occur (Table 1).

2.6 Fracture mechanisms of offset rock joints under uniaxial loading

Mughieda *et al.* (2004) has investigated the Fracture mechanisms of offset rock joints under uniaxial loading (Fig. 14). The inclination angle of the joints (β) remained constant at 45° for all specimens and the inclination angle of the bridge (α) was changed from 0.0° - 120° with an increment of 15° . The ratio of rock bridge surface to total shear surface was 0.6 ($K=0.6$).

In all specimens, the wing cracks were initiated and propagated before the failure, due to high concentration of tensile stresses at the joint tips. Mode of failure was dependent on the crack-

bridge configuration (Figs. 14(b)-14(d)). Bridge inclination was the main variable that controlled the mode of failure. For bridge inclination of 30° , 45° , 90° , and 105° , the coalescence occurred due to mixed tensile and shearing failures. For bridge inclination of 60° , 75° and 120° , coalescence was due to pure tensile failure. For non-overlapped joints, the strength of specimens was the highest for coplanar joints and the lowest for bridge inclination angle of 30° . Mixed mode of failure controlled the strength of offset joints. For overlapped joints, the strength increased as the bridge inclination angle increased. Difference in displacement between the bridge and the joint proves that there was progressive failure. In this research, the effect of confining pressure on the shear behaviour of rock bridge are ambiguous. Also, the effect of joint persistency on the failure pattern has been eliminated.

2.7 Experimental study of fracture coalescence in specimens (PMMA, Diastone, and granite) specimens consisting two flaw under uniaxial condition

Lee *et al.* (2011) have studied the experimental and numerical study of fracture coalescence in specimens consisting two flaws under uniaxial condition. The flaw geometry in a double-flawed specimen was combination of a horizontal flaw and an underneath inclined flaw as shown in Fig. 15 under uniaxial compression. The tests were performed on three different materials such as the PMMA, Diastone, and Hwangdeung granite specimens (Fig. 16).

The results shows that only tensile cracks were observed in the PMMA specimens, where coalescence occurred between the adjacent tips when α was smaller than 60° . With increasing α , the coalescence point moved from the upper tip of the inclined flaw to the lower tip of the inclined flaw.

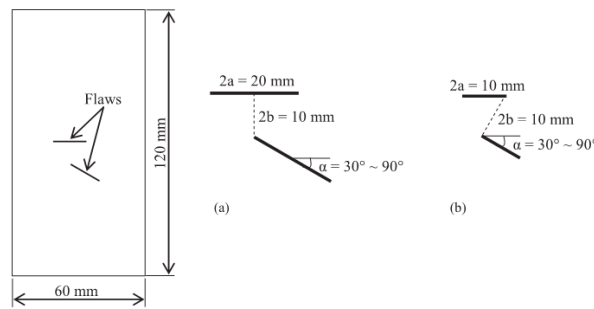


Fig. 15 Schematic plane view of the double-flawed specimen with the flaw geometry: (a) flaw geometry in PMMA and Hwangdeung granite specimens and (b) flaw geometry in Diastone specimens

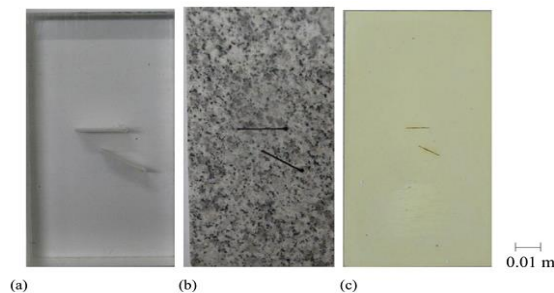


Fig. 16 View of the specimens: (a) PMMA and (b) Hwangdeung granite, and (c) Diastone

Shear cracks and tensile cracks were observed in the Diastone and Hwangdeung granite specimens. The shear cracks were observed after the tensile cracks emerged and caused the specimen failure. A white patch was observed in the Hwang-deung granite specimens, which showed a precedent phenomenon before the crack initiated at that place. However, cracks did not always appear at a place where the white patch emerged. Cracks of ten appeared without any signs of whitening, even though a white patch propagated from the same tip in a different direction.

2.8 Coalescence of offset rock joints under biaxial loading

Mughieda *et al.* (2006) has investigated the Coalescence of offset rock joints under biaxial loading (Fig. 17). Inclination angle of the joints (β) remained constant at 45° for all specimens and inclination angle of the bridge (α) was changed from 0 to 90° with an increment of 15 . The specimens were tested under three different confining stresses: 0.35 , 0.7 and 1.5 MPa, and the lateral stress to unconfined compressive strength (11 MPa is an average value) ratios were: 0.032 , 0.064 and 0.14 , respectively.

Experimental study proved that, the coalescence mechanism and the strength of jointed blocks with open offset rock joints were highly dependent on the bridge inclination angle (Fig. 18). In all specimens, wing cracks initiated and propagated before the failure due to high concentration of tensile stresses at the joint tips. For low confining stress, wing cracks appeared in the middle of joints. The mode of failure was dependent on the crack-bridge configuration.

Bridge inclination was the main variable that controlled the mode of failure. For bridge inclination of 0° , the coalescence occurred due to shear failure and for bridge inclination of 90° , the coalescence occurred due to tensile failure while for the other bridge inclinations, coalescence occurred due to mixed tensile and shear failure. Results showed that for non-overlapped joints, the strength of specimens was the highest for coplanar joints and the lowest for bridge inclination angle of 30° . Mixed mode of failure controlled the strength of offset joints. In this research, the effect of confining pressure has been investigated only in two directions. Also, the effect of joint persistency on the failure pattern has been eliminated. In this research dimension of sample is small and scale effect was absent in the research.

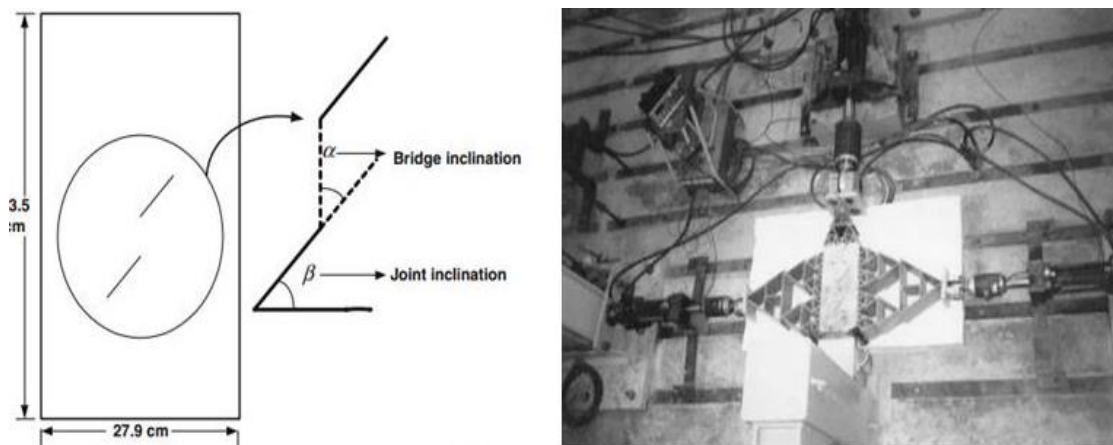


Fig. 17 (a) Geometry of specimens and the pre-existing cracks and (b) Biaxial testing equipment, general set-up, Mughieda *et al.* (2006)

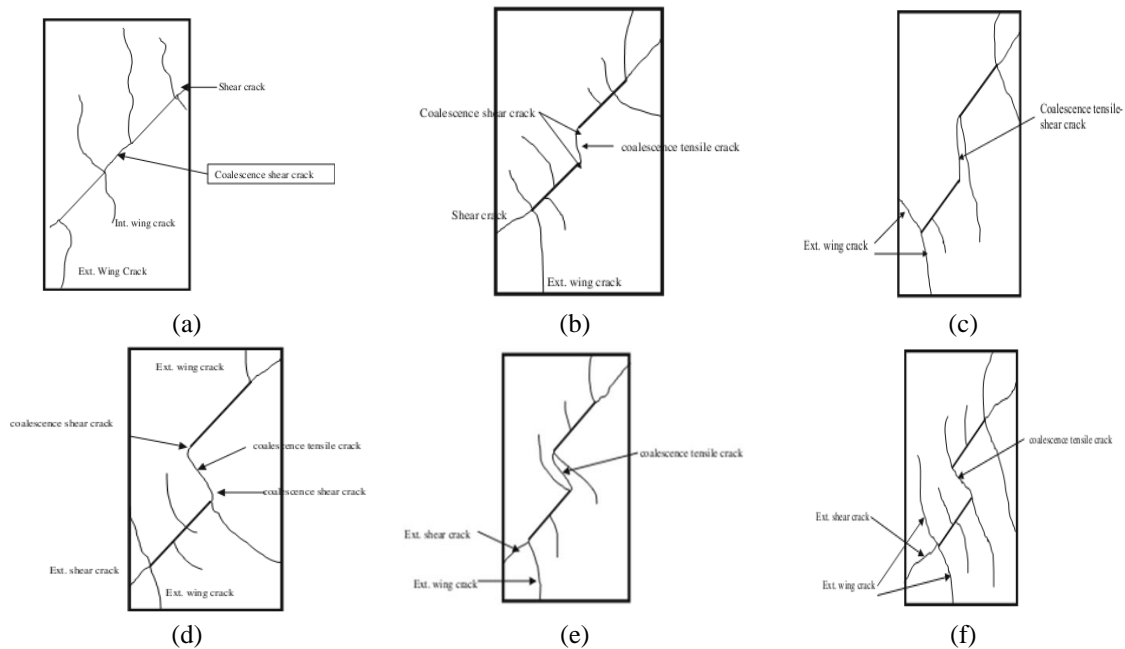


Fig. 18 The coalescence mechanism of open offset rock joints

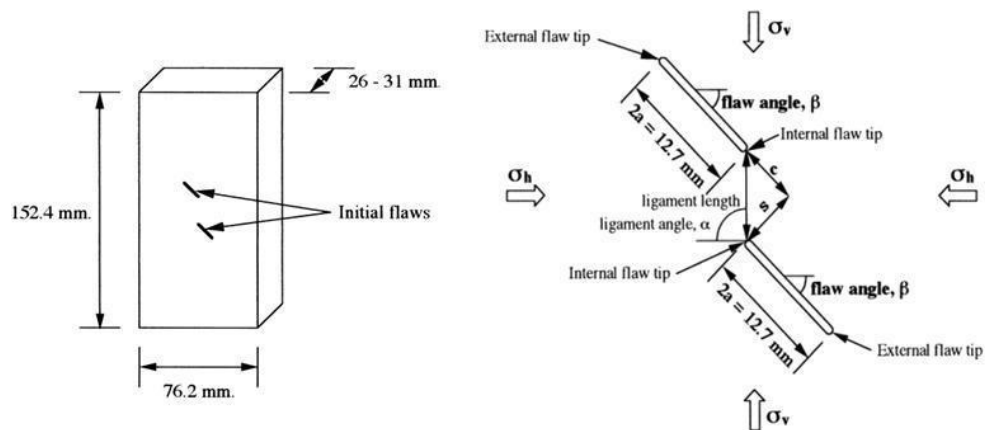


Fig. 19 Geometries of model rock specimen. (a) Overall view and (b) detail, Bobet and Einstein (1998)

2.9 The fracturing coalescence in rock type material under uniaxial and biaxial compression

Bobet and Einstein (1998) have investigated the fracturing coalescence in rock type material under uniaxial and biaxial compression (Fig. 19). the flaw angles (β) were set at 30° , 45° and 60° , the spacing (s) was 0 to $4a$ and the continuity (c) was from a to $4a$. The flaw types were either open or closed. Results showed that by increasing confining stresses, wing cracks initiations which were expected to occur at flaw tips shifted towards middles of the flaws. Secondary cracks which in some cases were actually appeared before the wing cracks, involved in cracking coalescence.

Both types of cracks grow stably to a point before the coalescence, when unstable propagation of secondary cracks takes place. A very interesting observation relates to the influence of ligament length is, i.e., distance between the flaws. Up to a distance of 1.5 times of the flaw length, flaws effect on each other during the crack growth; also coalescence can only occur if flaws are sufficiently close to each other, a distance which decrease with increasing confining stress. It is also significant to mention that, the secondary cracks initially propagate in shear in many cases up to the coalescence. In this research, the effect of confining pressure has been investigated only in two directions. Also, the effect of joint persistency on the failure pattern has been eliminated. In this research dimension of sample is small and scale effect was absent in the research. It's to be note that the spacing and continuity of rock joint have important effect on the failure behaviour but this effect has been eliminated due to small scale of sample.

2.10 Scale effect on engineering properties of open non-persistent rock joints under uniaxial loading

Mughieda *et al.* (2004) has investigated the scale effect on engineering properties of open non-persistent rock joints under uniaxial loading (Fig. 20). Uniaxial compression tests were performed on blocks made of rock like material. Three block sizes were tested having dimensions of (63.5×28×20.3) cm, (40.7×20.3×13.5) cm and (30.5×15.24×10) cm with different degrees of persistence (K) (joint length percentage of the total non-persistent length; 0.2, 0.4, 0.6 and 0.8) and joint angle. Joint angles (β) were set at 45° or 67.5°.

Results showed that there are two modes of failure; shearing failure along the non-persistent joints, and the failure through intact materials, depending upon the following three factors: As β increases, mode of failure changes from failure through intact material to shearing along the non-persistent joints. As K increases, the mode of failure tends to change from splitting failure in intact materials to shear failure along the planes of non-persistent joints. As sample size decreases, the mode of failure changes from splitting failure in intact materials to shearing failure along the planes of non-persistent joints. As size increases, strength decreases. In this research, the effect of confining pressure on the shear behaviour of rock bridge is ambiguous. Also, the effect of number of joints on the failure pattern has been eliminated.

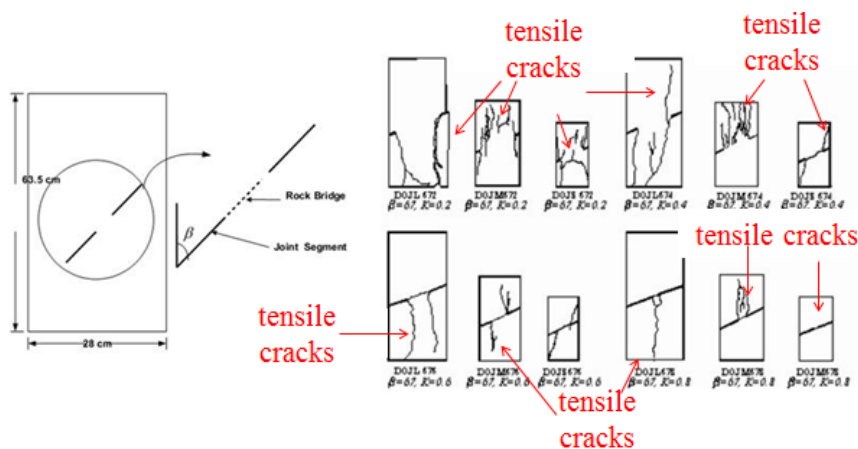


Fig. 20 Scale effect on the mode of failure, $\beta=67^\circ$, Mughieda *et al.* (2004)

2.11 Coalescence of three rock joints under uniaxial loading

Since in rock masses, a number of discontinuities are present, the question remains as whether the observations from specimens with two flaws can be extrapolated to specimens with multiple flaws.

Lin *et al.* (2000) and Wong *et al.* (2000) reported very briefly the results from specimens containing multiple flaws under both uniaxial and biaxial compression. Number of flaws in specimens was from 3 to 42. To study the failure of brittle rocks consisting non-persistent joints,

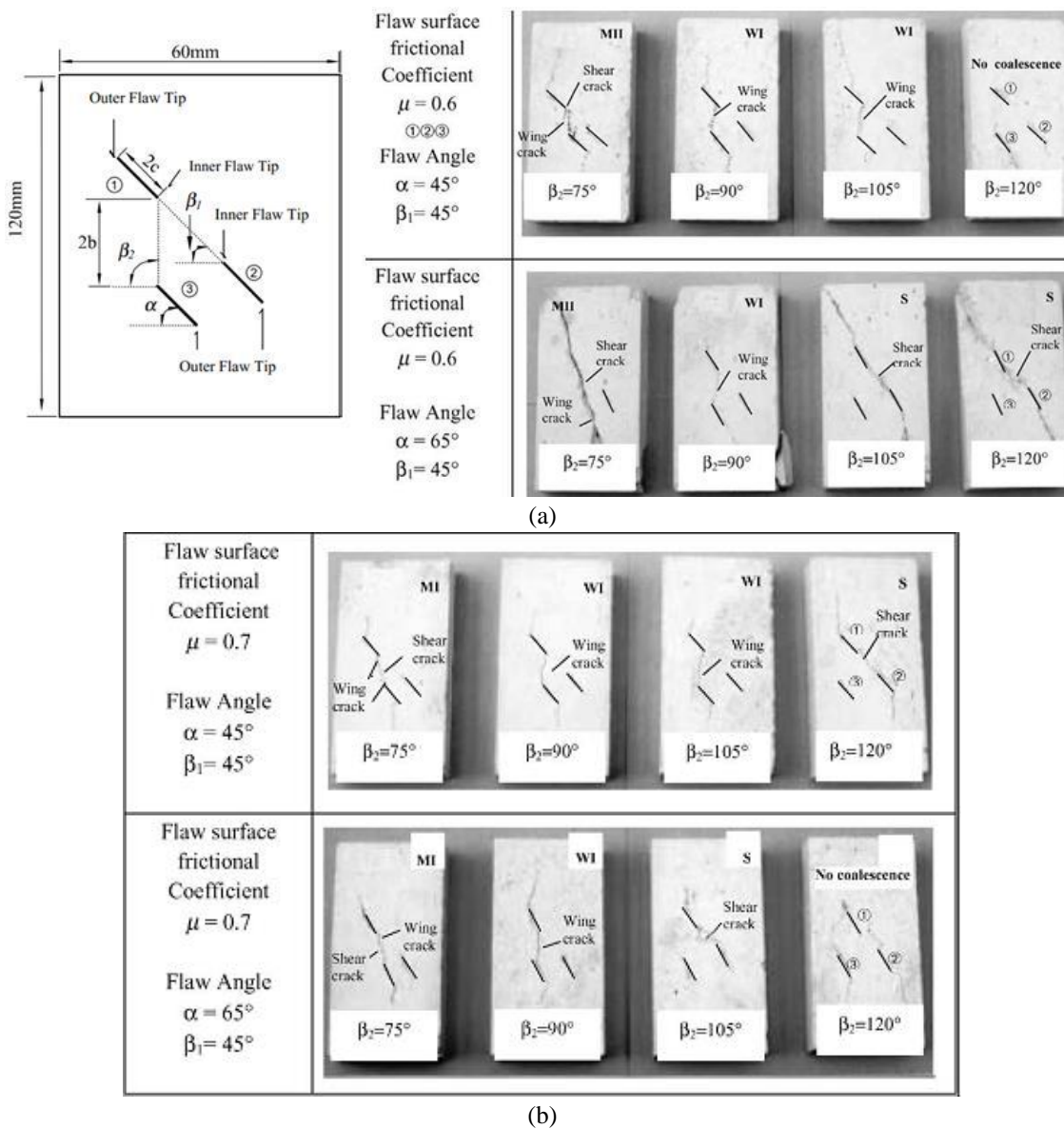


Fig. 21 The specimen containing three flaws, (a) $\mu=0.6$ and (b) $\mu=0.7$. Wong *et al.* (2001)

Nemat-Nasser and Horii (1982), Horii and Nemat-Nasser (1985, 1986) investigated the mechanism of crack interactions and the final failure patterns in fractured (flawed) plates made of Columbia resin CR39 under uniaxial, as well as biaxial compressions. Their specimens contain a series of flaws of different lengths and orientations (Horii *et al.* 1985). They showed that the flaw length is one of the parameters controlling failure patterns specimens. In general, larger flaws control mechanism of coalescence in the form of axial splitting under uniaxial compression with little or no crack growth from small flaws. Under biaxial compression, the growth of larger flaws is followed by the growth of smaller flaws and the final failure is a coalescence of smaller flaws in a form of shear zone or fault. Wong *et al.* (2001) investigated the crack coalescence in rock-like materials containing three flaws (Fig. 21). The inclinations of the pre-existing flaws α used in this study were 45° and 65° . The bridge angle of β was fixed at 45° , while α varied from 75° to 120° . Length of flaw $2c$ was fixed at 12 mm. Bridge distance between the two flaws $2b$ was fixed at 20 mm.

Results show that the crack coalescence occurs between only two flaws (not three). The mechanisms of crack coalescence depend on coalescence stress of the pair of flaws. The lower value of coalescence stress between the pair of flaws will dominate the process of coalescence. Mixed and wing tensile modes of coalescence are more likely to occur in respect to the shear mode, if coalescence stress between a pair of flaws be very close to (within 5% of each other). Frictional coefficient m of flaw surface can affect the pattern of coalescence of cracked solids. Uniaxial peak strength for cracked specimens does not depend on the total number of flaws but only on the number of flaws which actually involved in forming shear zone of failure pattern. In this research, the effect of confining pressure on the shear behaviour of rock bridge is ambiguous. Also, the effect of number of joints on the failure pattern has been eliminated. It's to be note that the behaviour of sample consisting rock joint with various direction is ambiguous.

kuntz *et al.* (1998) has used the steady-state flow experiments to visualise the stress field and potential crack trajectories in a 2D elastic-brittle cracked media for uniaxial compression. Several experiments with one single, two en-echelon and randomly distributed cracks have been conducted and compared with analogue data in two-dimensional elastic plates. It is shown that the steady state flow method not only provides an accurate picture of crack-induced perturbation of the displacement field but may also be used to predict the potential trajectories of mode I cracks. Micro mechanisms of the cracks interactions such as screening or enhancing effects are well illustrated. Since the coalescence is observed only for few favourable initial configurations of pre-existing flaws, the emergence of a macroscopic failure still remains an open question.

2.12 Coalescence of pre-cracked specimens under uniaxial loading

Sagong *et al.* (2002) have conducted a number of experiments on pre-cracked specimens, made of gypsum loaded in compression (Fig. 22).

Two series of tests have been investigated: specimens with three flaws, and with 16 flaws. The objective of their research is to ascertain if the crack types and coalescence patterns produced in specimens with two flaws can be extrapolated to specimens with three and 16 flaws. Three parameters are changed to produce different geometries (Fig. 8(b)): flaw inclination angle, β ; spacing, S ; and continuity, C : All flaws were parallel to each other and have the same angle β with the Horizontal (i.e., the horizontal is defined as perpendicular to the direction of loading). Three flaw inclination angles were at: 30° , 45° , and 60° . Spacing, S ; is the distance between the two contiguous rows of flaws, and is measured along a direction perpendicular to the planes of the

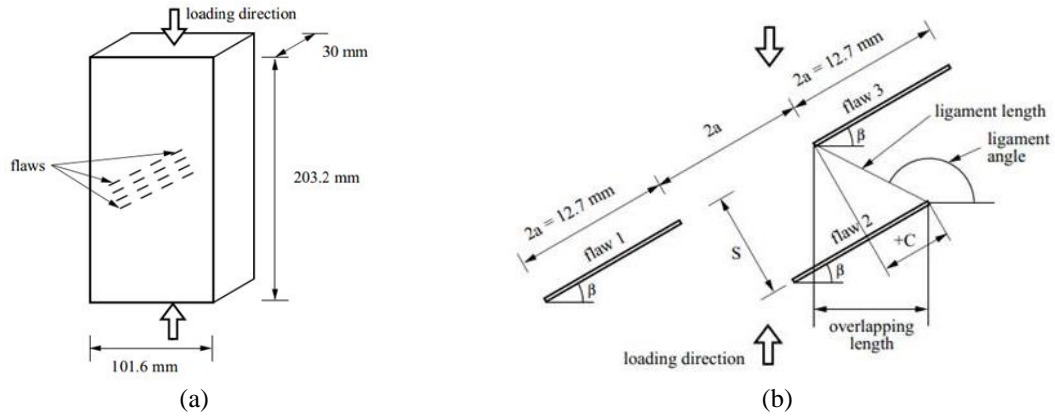


Fig. 22 Specimen with multiple flaws, (a) Overall view and (b) geometry of the flaws, Sagong *et al.* (2002)

flaws. Two different spacing are used; a , and $2a$ (i.e., 6.35 and 12.7 mm); $2a$ refers to the length of flaw, and a , half-length of flaw; all flaws had the same length, $2a=12.7$ mm). Continuity, C ; is the distance between the flaws in two different rows, and is defined as the overlapping length between two flaws measured along the planes of the flaws (see Fig. 22(b)). Continuity can be positive (as in Fig. 22(b)), or negative (for example, if the right tip of flaw 2 (one side of the crack) in the Figure is between flaw 1 and flaw 3). Five investigated continuities were: $-2a$, $-a$, 0 , a , and $2a$ (i.e., -12.7, -6.35, 0, 6.35 and 12.7 mm). Distance between flaws on the same row was kept constant for all tests and equal to $2a$ (12.7 mm; see Fig. 22(b)).

Results showed that the initiation stresses for wing crack and secondary crack were dependent on the geometry of flaws. Initiation stress increases with; the flaw angle, the spacing, the overlapping ratio, and decreases with the number of flaws.

Coalescence was produced by the linkage of two flaws through wing and/or secondary cracks. Linkage can be produced by any combinations of wing cracks and secondary cracks. Nine types of coalescence have been identified based on the nature of the cracks involved. Type of coalescence can be correlated with the geometry of flaws, defined by the flaw inclination angle and the ligament angle. Coalescence Type I occurs in coplanar flaws; coalescence Type II in non-overlapping left stepping flaws; coalescence Type IV in overlapping left stepping flaws; coalescence Type III is a transition between Types II and IV (i.e., transition between non-overlapping and overlapping); coalescence Type V for perfectly overlapping geometries; coalescence Type VI for overlapping right stepping geometries; coalescence Types VIII and IX for non-overlapping right stepping geometries; coalescence Type VII is a transition between Types VI and VIII (i.e., between overlapping and non-overlapping) (Fig. 23).

Coalescence stress increases with flaw inclination angle and ligament length. For ligament lengths greater than $3a$, the joint length would be $2a$ and the coalescence stress stays constant and it is rather independent of the relative locations of flaws. Coalescence in specimens with multiple flaws tends to occur in a “columnar” pattern where flaws in the same column are linked together.

The right and left stepping failures observed in three flaws samples occurred for the samples consisting 16 flaws too (Fig. 24).

In this research, the effect of confining pressure on the shear behaviour of rock bridge is ambiguous. Also, the behaviour of sample consisting rock joint with different direction is unknown.

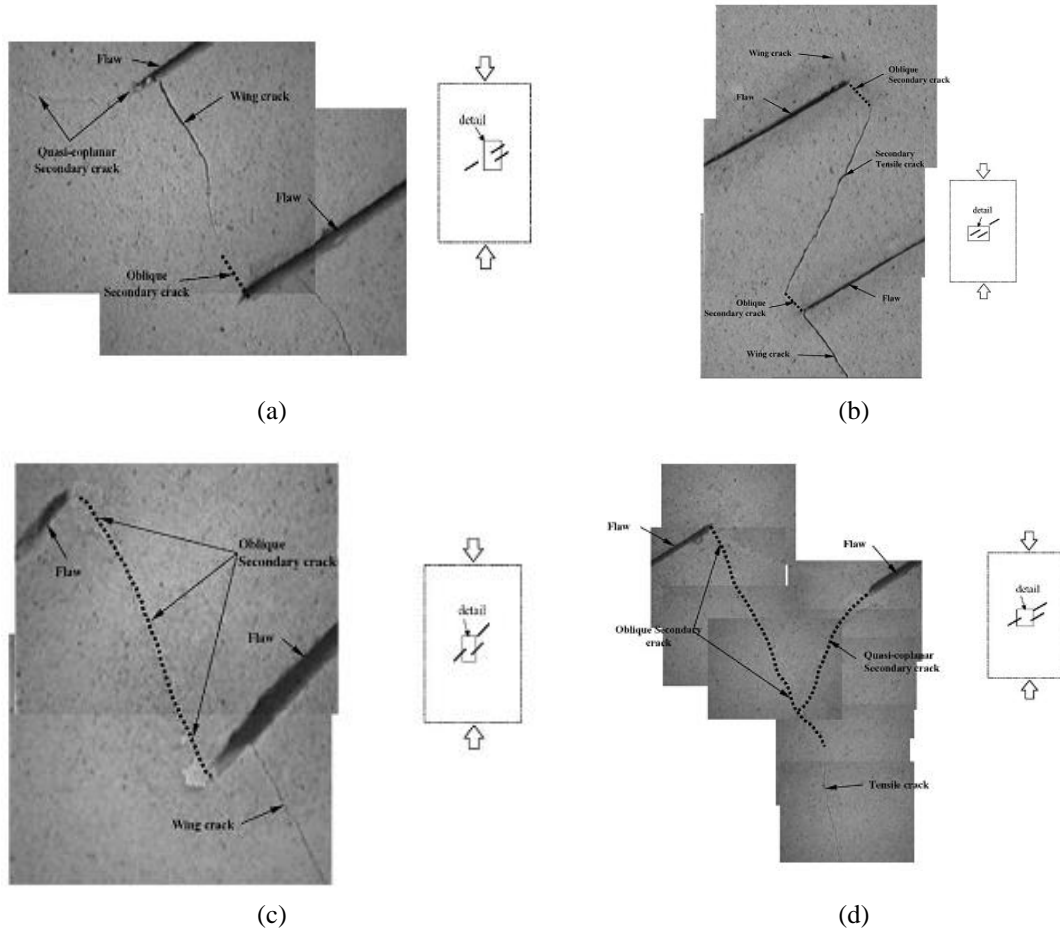


Fig. 23 Crack coalescence in different samples, (a) Type VI. Specimen a2a30°, (b) Type VII. Specimen aa30°, (c) Type VIII. Specimen a045° and (d) Type IX. Specimen Aa30°

Type	Left Stepping	Type	Right Stepping
I		VI	
III		VII	

Fig. 24 Coalescence in specimens with multiple flaws

It's to be note that the result of this research was restricted to gypsum. It's important to clarify what is the behaviour of rock bridge when inserted in different materials.

2.13 Failure modes of rock mass models with parallel non-persistent joints

Prudencio *et al.* (2007) has investigated the strength and the failure modes of rock mass models with non-persistent joints (Fig. 25). Joint geometries and confining stresses are shown in Table 2. Results show that, stress orientation relative to joint orientation and the value of confining stress are concluded from different failure modes. Samples with steeply dipping non-persistent joints and the joint step angles larger than 90° underwent planar failure. Strengths of some samples turned out to be larger than those predicted by a simple model, because normal stress on rock bridges is several times larger than that assumed by simple (intact) model. Low confining pressures when the joint step angle is approximately 90° can induce a step failure along an average slope angle of $\psi_f = \psi_1 + \Delta\psi$, where ψ_1 is the dip of joint system and $\Delta\psi = \tan^{-1}(d/L_j)$ (d is the joint spacing and L_j is the joint length).

Table 2 Joint geometries and confining stresses of the samples tested, Prudencio *et al.* (2007)

Series	L_j (cm)	L_r (cm)	D (cm)	γ'	β°	E (cm)	$\frac{\sigma_2}{\sigma_c}$								
1	5	2	2			0.01	0	0.05	0.169						
2				90	45		0	0.026	0.04	0.05	0.096				
3				135	15		0	0.043	0.047	0.103	0.169				
4					30		0	0.017	0.023	0.053	0.091	0.103	0.169		
5					45		0	0.04	0.064	0.126					
6					60		0	0.011	0.025	0.035	0.06	0.077	0.079	0.176	0.199
7			4	117			0								
8		3		127	45		0	0.011	0.02	0.039	0.058	0.086			
9		2	2	112.5			0	0.03	0.055	0.075	0.1				
10				135		0	0	0.042	0.066	0.123					
11	2.5	1	1	90		0.01	0	0.099							

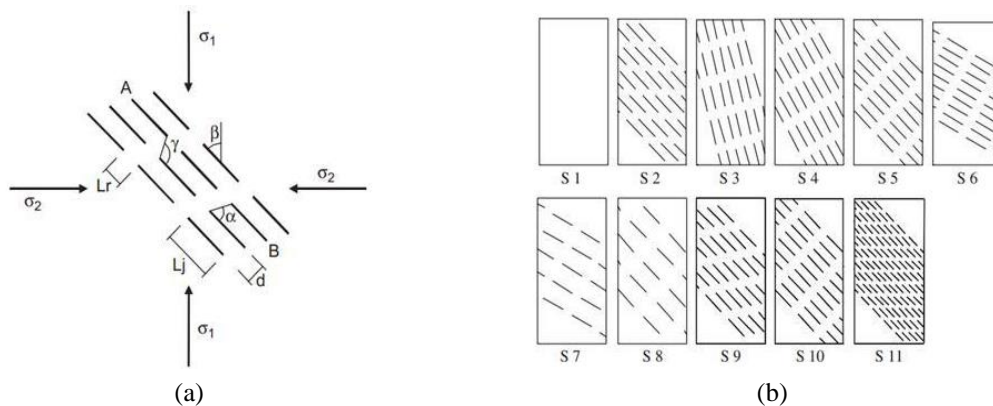


Fig. 25(a) Parameters varied in the tests and (b) Joint geometries tested, Prudencio *et al.* (2007)

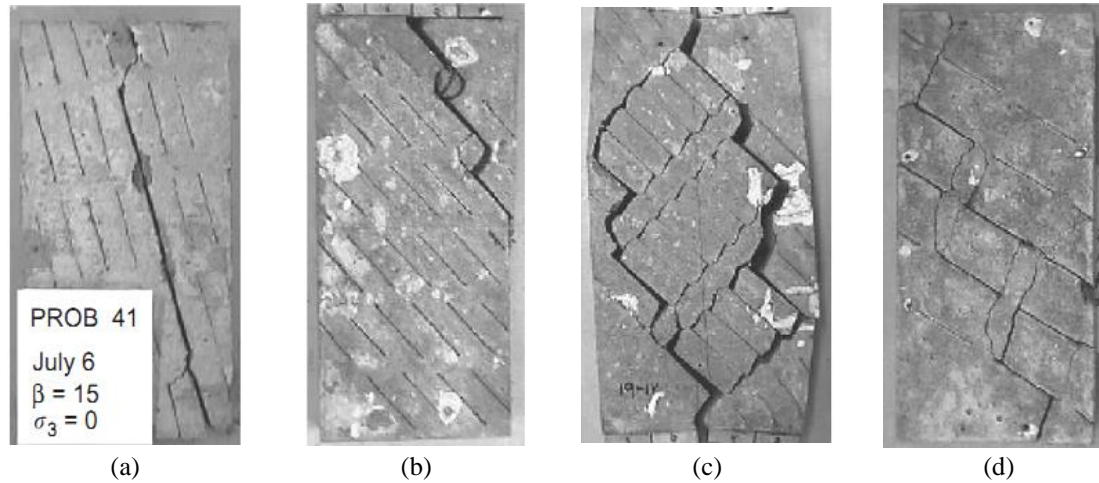


Fig. 26 Observed failure modes: (a) through a plane, s3, $\sigma_2/\sigma_c=0.0$, (b) stepped, s2, $\sigma_2/\sigma_c=0.0$, (c) rotation of new blocks s5, $\sigma_2/\sigma_c=0.0$ and (d) interaction between rotation and stepped, s8, $\sigma_2/\sigma_c=0.01$

Wing fractures and tensile failure propagating in the rock bridge between the parallel adjacent fractures can significantly reduce the strength of rock mass. As a result, the model divides into a series of individual blocks which can rotate, leading to a toppling or “rotational failure”. The overall strength can be as low as the residual strength on an equivalent joint along the potential failure surface. Planar failure and stepped failure are associated with higher strengths, brittle behaviour, and small failure strains, while rotational failure is usually associated with a very low strength, ductile behaviour, and large deformation. The ability to forecast failure mode has a significant economic effect on open pits stabilities: rotational failure would lead to a regressive slope failure, while a planar failure, although associated with a possible steeper pit, would lead to a brittle behaviour of the slope (Fig. 26).

In this research, the effect of confining pressure has been investigated only in two directions. Also, the effect of joint persistency on the failure pattern has been eliminated due to restrict in sample dimension. In this research sample is small. Scale effect was absent in the research.

2.14 Rock-like material with pre-cracks under uniaxial compression

Wen *et al.* (2013) have studied the experimental study on rock-like material with pre-cracks under uniaxial compression (Fig. 27).

The stripes of pre-crack are as follows: 6 stripes, 9 stripes, 12 stripes, 15 stripes, 18 stripes, and the crack's angle contents $15^\circ, 30^\circ, 45^\circ, 60^\circ$, the length of crack is 2 cm. Combined the number and the angle of crack, 20 specimens in total with different crack stripes and different crack angle were made (Fig. 28).

Results show that the crack extended grossly from up to down, left to right. The crack initiated from top left corner of specimen because of tension stress concentration, then the wing crack was formed, the wing crack connect the vertical pre-cracks, the rock bridge left side damaged. Also, middle pre-crack was connected by tension failure, the secondary shear crack between pre-cracks transfixied the specimen because of the action of shear. And the secondary shear crack connected the two main cracks: the middle and the right. The damage of rock bridge and the transfixion of

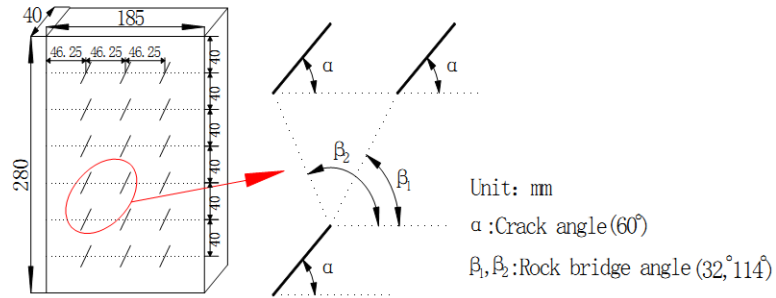


Fig. 27 The spatial arrangement of rock like material with 18 stripes



Fig. 28 The part of real specimens

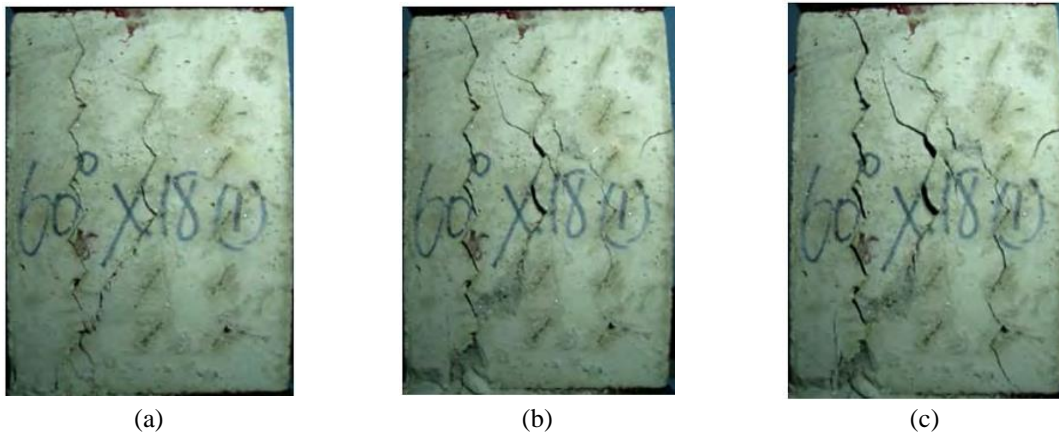


Fig. 29(a) The failure prophase of rock like material specimen with $60^\circ \times 18$ stripes, (b) the middle failure stage of rock like material specimen with $60^\circ \times 18$ stripes and (c) the late failure stage of rock like material specimen with $60^\circ \times 18$ stripes

pre-crack gave rise to the failure of specimen. Besides, wing crack is the main transfixion mode of specimen (Fig. 29).

2.15 Creeping damage around an opening in rock-like material containing non-persistent joints

Wong *et al.* (2002) has investigated creeping damage around an opening in rock-like material containing non-persistent joints (Fig. 30). The locations and orientations of slots are pre-determined by giving a fixed arrangement of joints. The lengths ($2c$) and the angles of joints are fixed at 10 mm and at 45° , respectively. Lengths of the three bridges (the distance between the two joints, i.e., B_1 , B_2 , B_3) are fixed at 10 mm. For all specimens, the angle of bridge β_2 or β_3 is fixed at 105° while the bridge angle for β_1 at 45° . Two types of stress levels are applied on the jointed specimen with an opening, to study the creeping damage after excavation. For the first type stress level, the σ_3 value is changed with a fixed stress of σ_1 . The fixed σ_1 is set at 1.2 MPa, at 65% of σ_{1max} . This fixed σ_1 (1.2 MPa) is the average stress level required to cause crack initiation in jointed specimen. The σ_3 changes is varied from λ (σ_3/σ_1)=1/3 to 1 with 1/6 increment. Second type of stress level is based on the changes of σ_1 with a fixed λ value. The σ_1 is changed from 45% to 85% of σ_{1max} with 20% increment. Thus, applied σ_1 are changed from 0.8, 1.2 to 1.6 MPa. These three stress levels represent the stress below, at, and above the crack initiation stress. With a fixed λ , the applied σ_3 will also be varied with the changes in σ_1 . For a systemic studying on creeping around the excavated opening, the λ value is also varied from 1/3 to 1. With these variations, the effects of in situ stress level on failure mechanisms and the creeping time to failure could have been fully studied.

Results show that, when the stress ratio $\lambda(\sigma_3/\sigma_1)$ is low (1/3) (Fig. 31(a)), the tensile mode of creeping failure is dominant and with high stress ratios of ($\lambda > 1/2$), the shear mode or a combined tensile and shear mode are (Figs. 31(b) and 31(c)).

For a lower $\lambda(\lambda \leq 1/3)$, the micro-fractures are induced and propagate stably towards the neighbouring joints, opening with a stepwise increasing until final failure. For a higher $\lambda(\lambda > 1/2)$, deformation around the opening fluctuate slightly after the excavation, then sudden failure. For $\lambda > 2/3$, no deformation changes after the excavation momentarily, then sudden failure. Deformation around the opening decreases distance away from it where the strain of the inner zone ($r \leq 1.7 a$) is about four times larger than that of the strain in the outer zone ($r > 1.7 a$). For a high stress ratio of $\sigma_1/\sigma_{1max} > 65\%$ (σ_{1max} : the peak stress of jointed rock-like specimen without

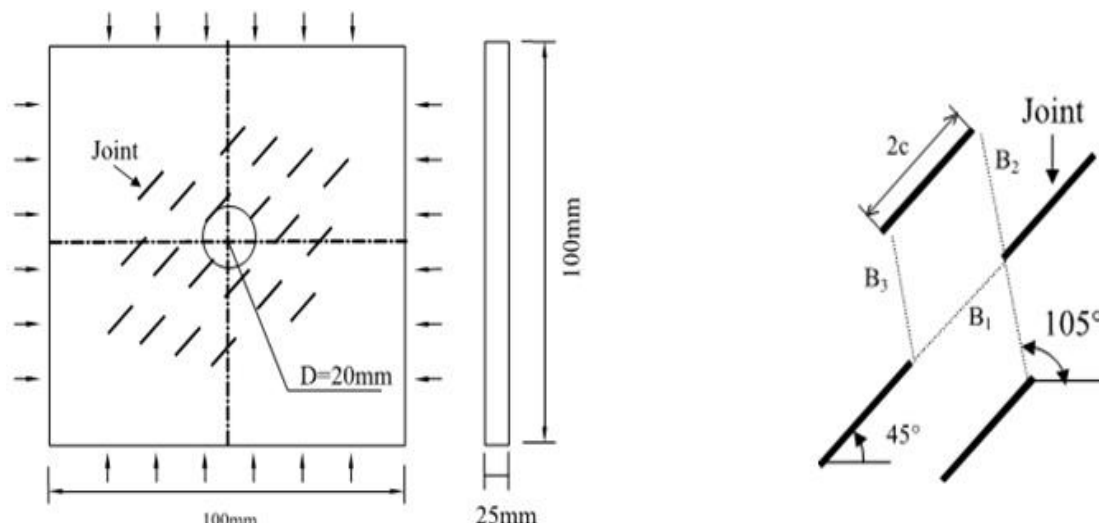


Fig. 30 Geometry of model rock-like specimen. B_1 , B_2 and B_3 are the distance between two joints, Wong *et al.* (2002)

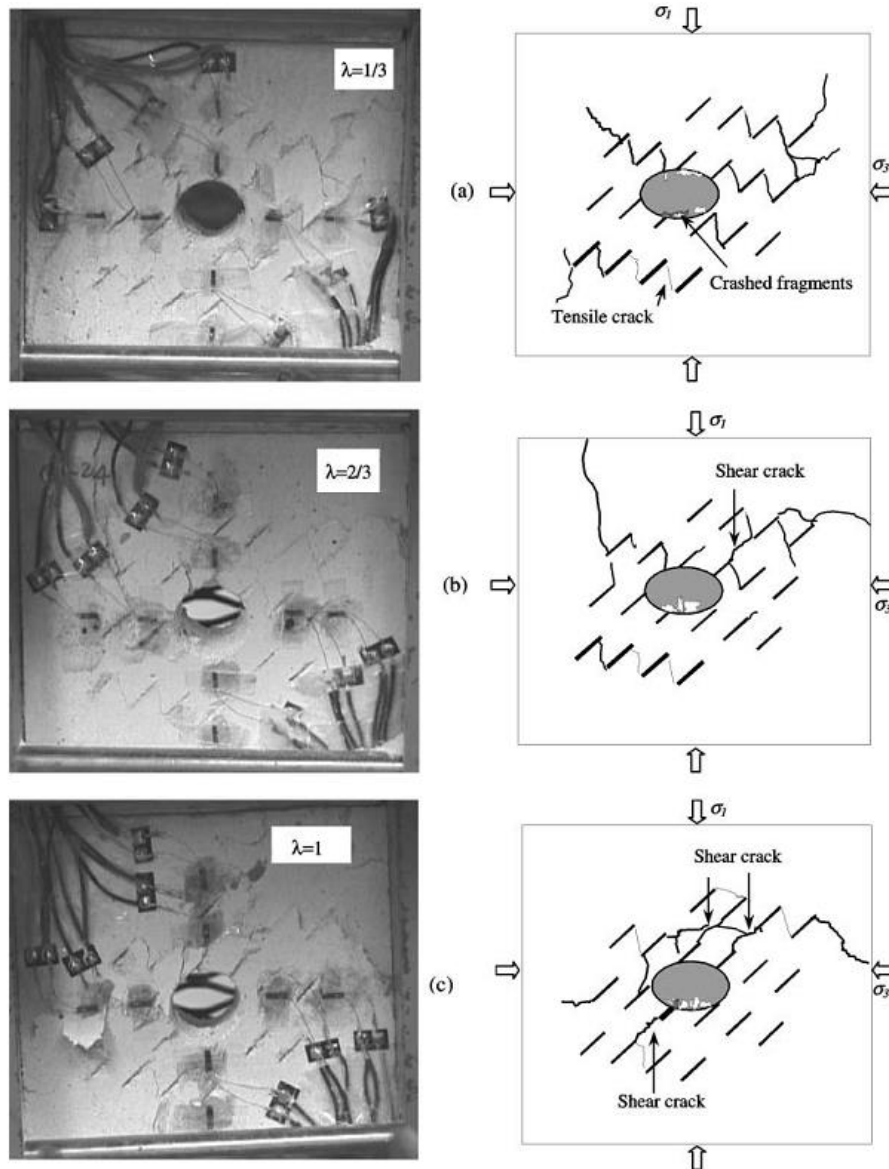


Fig. 31 Failure pattern in different samples, (a) $\lambda=1/3$ and (b) $\lambda=2/3, \lambda=1$

opening), large deformation appears after the excavation. As a result, faster collapses of the opening will occur. When $\sigma_1/\sigma_{1max} < 45\%$, only few cracks initiate and propagate after the opening was drilled. As a result, the opening remains stable. Creeping failure time decreases with an increase in stress ratio of λ and σ_1/σ_{1max} . Stress ratios λ and σ_1/σ_{1max} are important indices indicating the degree of instability of an opening after excavation.

In this research, the effect of confining pressure has been investigated only in two directions. Also, the effect of joint persistency on the failure pattern has been eliminated due to restrict in sample dimension. In this research sample is small. Scale effect was absent in the research.

The effect of tunnel diameter on failure behaviour is unknown. In this research the effect of porosity, density, material mixture has been eliminated.

2.16 Rock slope failure containing a lot of rock bridges

Rocky landslides contain a lot of rock bridges, and researches on rock bridge were carried out by experimental methods and simulated by analytical and numerical simulation techniques. The laboratory study of AE characteristics during rock stress-strain process was reviewed (Rudajev *et al.* 2000, Jansen *et al.* 1993); real-time failure process (Wang *et al.* 2013) and stability evaluation and harm degree of landslides (Cheon 2011) were marked out. Behavior of rock bridge was observed firstly by shear test in 1990 (Li *et al.* 1990); then cyclic loading test of rock bridge and mechanical behaviour was carried out (Shen 1990). The failure mechanisms and pattern of coalescence of rock bridges were investigated (Wong 1999). Strength, deformability, failure behaviour, and AE locations of red sandstone were tested by using triaxial compression (Yang 2012). Analytical methods such as neural network (Ghazvinian 2010), slice element method (Zhang 2008), and time-dependent degradation failure (Kemeny 2005, Zhu *et al.* 2004) are used to study the progressive failure of rock bridge.

Chen *et al.* (2015) was investigated the failure mechanism of Rock Bridge based on acoustic emission technique under direct shear test (Fig. 32).

The results show that AE source location can be accurately located during small scale tests in small scale direct shear tests. The AE event count peak value increases with the increasing of rock bridge length and vertical stress. In addition, the time of AE event count peak value appearing goes back with the increase of the length and the vertical stress. AE resource location was accurately and reliably located during large scale landslide model test with locked section. Based on the locating process, rock sample failure features and cracks time-space evolution process were revealed. AE showed that the brittle failure feature of landslide with locked section was reflected well.

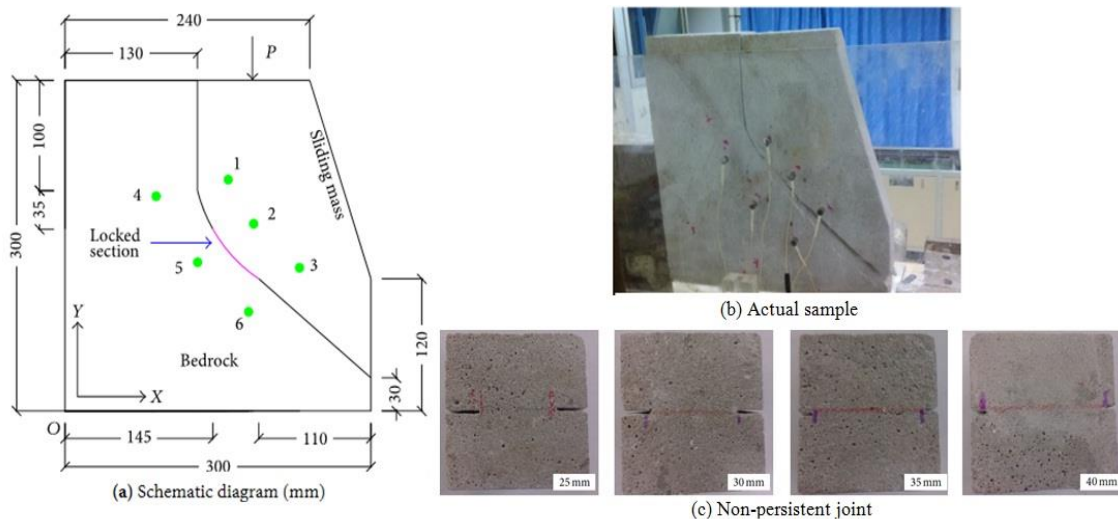


Fig. 32(a) Sample size and sensor position, (b) Failure of locked section under continuous loading and (c) Different reserved rock bridge length, Chen *et al.* (2015)

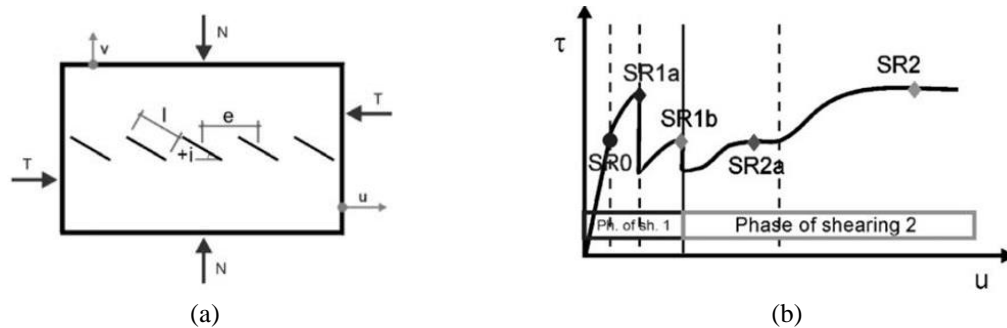


Fig. 33 (a) Shear specimen with discontinuous joint. Definition of the geometrical parameters and (b) beginning of idealized shear test record. Shear stress τ is shown to vary systematically with growing shear displacement u , Gehle (2003)

In this research the effect of echelon joint, joint roughness, joint filling and joint aperture on the failure behaviour has been eliminated. Also the effect of material mixture on the failure pattern is ambiguous.

However, most of the previous studies are focused on the mechanisms of crack initiation, propagation and interaction under uniaxial and biaxial compression, but relatively few experimental investigations were done to examine the pattern of crack coalescence in the rock bridge area under direct shear loading. Lajtai (1969a, b) performed direct shear testing on model material with non-persistent joints and observed that, the failure mode changes with increasing normal stress. He suggested a composite failure envelope to describe the transition from tensile strength of an intact material to residual strength of discontinuities. He thus recognized that the maximum shear strength develops only if strength of solid material and the joints are mobilized simultaneously. Savilahti *et al.* (1990) did some further study on the specimens with jointed rock under direct shear testing where the joint separation varies in both horizontal and vertical directions and joint arrangement changes from non-overlapping to overlapping using modelling material. The coalescence patterns for specimens indicated that, the jointed rock failed in mixed and tensile modes for non-overlapping and overlapping joint configurations, respectively. Wong *et al.* (2001) studied shear strength and failure pattern of rock-like models containing arrayed of open joints in both modelling plaster material and natural rocks under direct shear tests. Results showed that failure pattern was mainly controlled by the joint separation while shear strength of jointed rock depended mostly on the failure pattern. Ghazvinian *et al.* (2007) made a thorough analysis of the shear behaviour of the rock-bridges based on changes in the persistency of their area. The analysis proved that, the failure mode and mechanism were under continuity effect for rock-bridge.

2.17 Breakage and shear behaviour of intermittent rock joints

Gehle (2003) investigated breakage and shear behaviour of intermittent rock joints (Fig. 33).

The effect of crack angle i ; scale and degree of separation ($l=e$; with crack length l and crack distance) (see Fig. 33(a)), the influence of different crack types and conditions, the influence of normal loading as well as of the kind of loading (CNL versus CNS), and finally, the influence of different model materials on shear failure behaviour of rock bridges has been investigated. These tests revealed that shearing of such joints is characterized by several mechanisms, each responsible for a special kind of shear resistance. Three phases for shearing can be identified. The

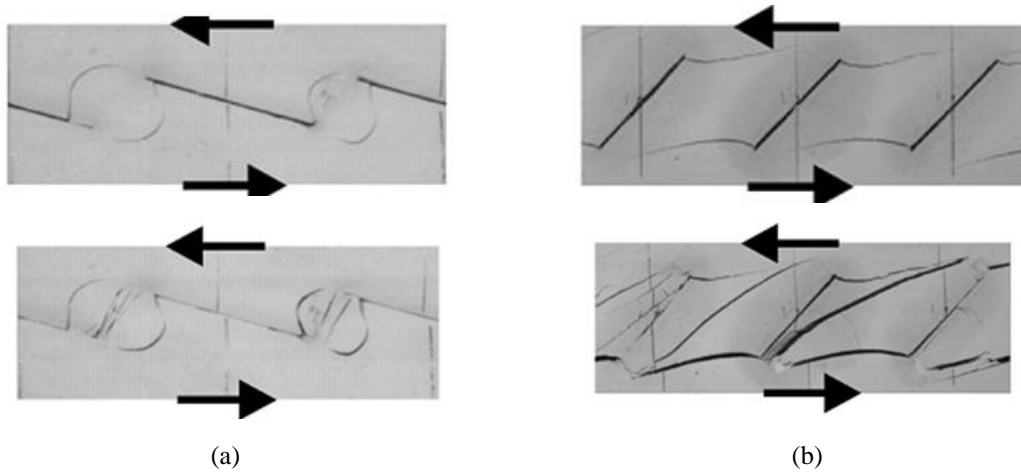


Fig. 34 Wing cracks grown at the first breakage incident (a) crack angle is 15° and (b) crack angle is 45°

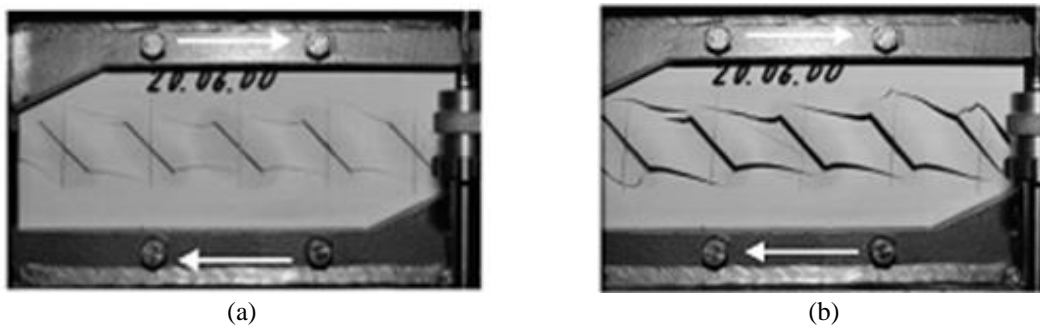


Fig. 35 Rotating mechanism of the rock bridges in the second phase of shearing (crack angle is 45°), (a) in the initiation of second phase and (b) at the end of second phase

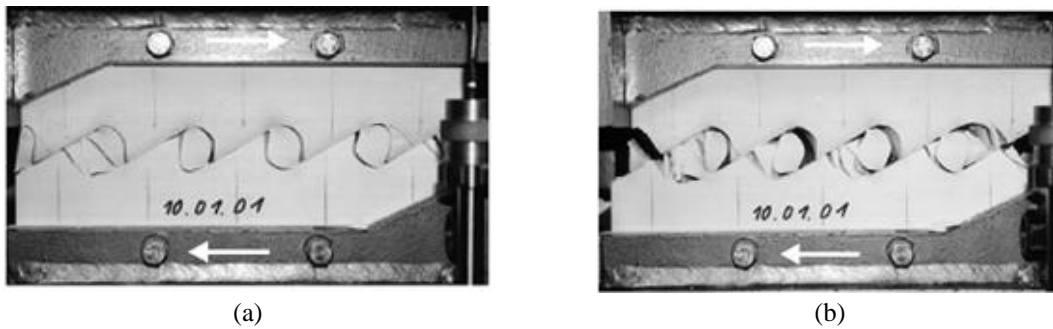


Fig. 36 Photographs of specimens with crack angle 30° during the course of the 2nd phase of shearing. Note that the initial cracks are closed or in contact, respectively. The change in the shape of the rotating rock fragments is directly noticeable at the shear resistance

characteristic or maximum shear resistances in these phases are called SR1 to SR3 (Fig. 33(b)). First shearing phase is that of actual rupture, initiated by the formation of wing cracks (at SR1a), starting from existing cracks and growing into the material bridges, and concluded by generating

additional new fractures connecting the initial cracks in the zone between the wing cracks (at SR1b) (Fig. 34). Complete bisecting of the material bridges is then obtained. The second phase of shearing is characterized by friction processes and volume increase in shear zone (Fig. 35).

Depending on whether or not the initial cracks are open, the shear resistances representing the levels in the shear curves are called SR2a or SR2.

Finally, the third phase of shearing, reached after large shear displacements, is determined by the sliding processes inside strongly fractured shear zone (Fig. 36). Here SR3 is the measured resistance.

These shear resistances corresponding to different shear mechanisms depend on various ways of testing conditions.

Each can be a maximum shear resistance, so none of the shear mechanisms may be neglected. Of all investigated parameters, the inclination of cracks inside discontinuous joint and the normal stress are found to have dominant effects on shear strength. Their influence varies from phase to phase due to different shear mechanisms. Each shear mechanism has been investigated in detail. Failure of the rock bridges by wing and connecting cracks are shown to be a tensile one. Frictional resistance after the completion of initially discontinuous joint is not only caused by sliding, but by rotation and further breakage as well. The final shear process is characterized by sliding within the rock breccia, into which the rock has been transformed by intensive cracking and crushing. Most important conclusion from the presented results is the fact that, not only one but several shear mechanisms are responsible for the shear strength of a discontinuous joint. Most previous models suggested that, evaluation of the shear strength of discontinuous rocks are usually based on one shear mechanism only or entirely empirical and are therefore not suited for the representation of complete shear process.

In this research the effect of joints persistency, joint number, scale effect, material mixture, echelon joint has been eliminated on the failure mechanism of non-persistent joint. Also the effect of normal load, loading rate, cyclic and dynamic loading are ambiguous on the shear behaviour of non-persistent joint.

2.18 The effect of joint overlapping on shear behaviour of rock bridge

Ghazvinian *et al.* (2011) has investigated the effect of joint overlapping on shear behaviour of rock bridge. Four specimens with similar Ligament length of 45 mm and different ligament angles of 0°, 25°, 90° and 115° were prepared (Ligament length is the distance between the tips of two joints and ligament angle is the counter-clockwise angle between the ligament length and shear axis. For different specimens, the lengths of edge joints were different but in same specimen, the lengths of those two joints were similar. The joint lengths (b) were at 52.5, 66.8, 75 and 78.8 mm, associated with the ligament angles of 0°, 25°, 90° and 115°; respectively.

All samples were tested by applying a shear displacement rate of 0.01 mm/s. Normal stress applied to the samples was set at 0.1 MPa. Observations showed that ligament angles influence failure pattern of the rock bridge. Fig. 36 shows four different types of failure pattern obtained in direct shear tests. When ligament angle is 0° (Fig. 37(a)), the upper tensile crack propagates through the intact portion area but the lower tensile crack develops for a short distance, and then becomes stable so as not to coalesce with the tip of other joint. When ligament angle is 25° (Fig. 37(b)), the wing cracks initiate at the tip of joints and propagate in curvilinear path till coalesce with the tip of other joint. This coalescence left an elliptical core completely separated from the sample. When ligament angle is 90° (Fig. 37(c)), the tensile crack initiates at the joint tip and

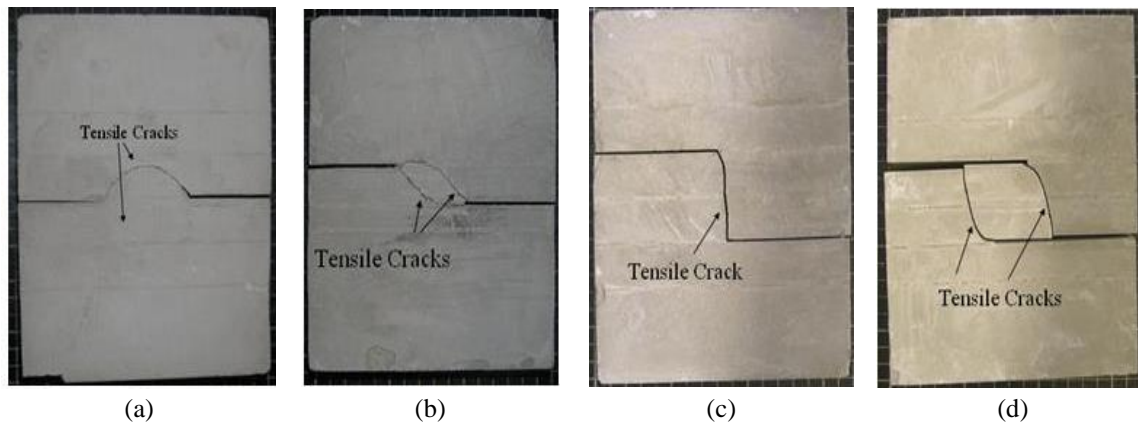


Fig. 37 The crack patterns for ligament angle of; (a) 0° , (b) 25° , (c) 90° and (d) 115° , Ghazvinian *et al.* (2011)

propagates through the bridged segment. In this configuration, the rock bridge is broken with a single failure surface. When ligament angle is 115° (Fig. 37(d)), the wing cracks initiate at joint walls and develop nearly in vertical direction. These wing cracks propagate through the intact portion area, till coalesce with the opposite joint tips. This coalescence leave a rectangular core of intact material completely separated from the sample. In these failure patterns, surface of failure at bridge area is tensile because no crushed or pulverized materials and no evidence of shear movement were noticed.

The models with ligament angle of 0° and 25° have the non-linear behaviour in force-displacement curve. The non-linearity in force-displacement curve means that, the wing cracks have a stable growth till the peak shear strength is reached. In other word, the wing cracks are suppressed by external normal stress so they have stable growth. When ligament angles are 90° and 115° , the load-displacement curve is completely linear. It means that, the wing cracks grow unstably as soon as they initiate between the joint.

Whereas, the effect of normal load is eliminated on the rock bridge due to joint overlapping, therefore the wing cracks grow unstably. Also results showed that, shear loading capacity of non-overlapped joints is more than that of overlapped joints due to normal load appearances on the rock bridge in non-overlapped joint configuration.

Results showed that, the failure pattern is highly dependent on joint overlapping. In non-overlapped joints, cracks were initiated from the joint tips and elliptical failure patterns occurred in the models.

In overlapped joints, the cracks were initiated from the joint walls and a rectangular failure patterns occurred in the models. Joint configuration had also been shown to affect the shear strength of non-persistent joints, so the shear strength of non-overlapped joints was more than that of the overlapped joints.

The amount of fracturing at the peak shear loading stage decreased with increasing the rock bridge angle. This means that, the length of stable crack growth decreases with increasing ligament angle.

In non-overlapped joints, the crack initiation stress was less than the failure stress, so progressive failure occurs, whereas for overlapped joints the crack initiation stress was equal to failure stress, so brittle failure occurred.

In this research the effect of joint number, scale effect, material mixture has been eliminated on the failure mechanism of non-persistent joint. Also the effect of loading rate, cyclic and dynamic loading are ambiguous on the shear behaviour of non-persistent joint.

3. Conclusions

The presence of rock bridges in not fully persistent natural discontinuity sets is a significant factor affecting the stability of rock structures. Compared with intact rocks, jointed rock masses are usually weaker, more deformable and highly anisotropic, depending upon the mechanical properties of each joint and the explicit joint positions.

Because of the inherent statistical nature and the uncertainties involved in the in situ survey of non-persistent joints, they are usually described by sets, hence by number of sets and the geometry of each set such as orientation, spacing and persistence. The fracture process of non-persistent joint can be divided into three main phases: The first phase of shearing is that of rock bridge rupture and model dilation, the second phase of shearing is characterized by friction processes and volume increase in the shear zone, finally, the third phase of shearing, reached after large shear displacements and determined by sliding processes inside the strongly fractured shear zone. These shear resistances corresponding to different shear mechanisms depend on various ways of testing conditions. Each can be the maximum shear resistance, so none of shear mechanisms may be neglected.

Researches show that, the bearing capacity of jointed rock decrease by increasing the number, the length and the inclination of non-persistent joint set. Coalescence in specimens with multiple flaws tends to occur in a “columnar” pattern where flaws in the same column are linked together. In fact the crack coalescence always occurs between the flaws for which the peak strength is lower.

The shear or mixed shear/tensile failure change to tensile failure by increasing the confining pressure, ligament length and ligament angle. Also, the bearing capacity of rock bridge increases by increasing the confining pressure. It means that, when non-persistent joint is situated in shallow area, it suppressed by low confining pressure so tensile failure occurs in the rock bridge. For non-persistent joint located in deep area, shear failure occurs in the rock bridge.

References

- Ashby, M.F. and Hallam, S.D. (1986), “The failure of brittle solids containing small cracks under compressive stress states”, *Acta Metall.*, **34**(3), 497-510.
- Batzle, M.L., Simmons, G. and Siegfried, R.W. (1980), “Microcrack closure in rocks under stress: Direct observation”, *J. Geophys. Res.*, **85**(B12), 7072-7090.
- Bieniawski, Z.T. (1967), “Mechanism of brittle fracture of rock Part II-experimental studies”, *J. Rock Mech. Min. Sci. Geomech. Abstr.*, **4**(4), 407-423.
- Bobet, A. (1997), “Fracture coalescence in rock materials: Experimental observations and numerical predictions”, Sc.D. Dissertation, MIT, Cambridge, U.S.A.
- Bobet, A. (2000), “The initiation of secondary cracks in compression”, *Eng. Fract. Mech.*, **66**(2), 187-219.
- Bobet, A. and Einstein, H.H. (1998), “Fracture coalescence in rock-type materials under uniaxial and biaxial compression”, *J. Rock Mech. Min. Sci.*, **35**(7), 863-889.
- Celestino, S.P., Piltner, R., Monteiro, P.J.M. and Ostertag, C.P. (2001), “Fracture mechanics of marble using a splitting tension test”, *J. Mater. Civil Eng.*, **13**(6), 407-411.

- Chen, G., Kemeny, J. and Harpalani, S. (1992), "Fracture propagation and coalescence in marble plates with pre-cut notches under compression", *Proceedings of the Symposium on Fractured and Jointed Rock Mass*, Lake Tahoe, California, U.S.A., June.
- Chen, G., Zhang, Y., Huang, R., Guo, F. and Zhang, G. (2015), "Failure mechanism of rock bridge based on acoustic emission technique", *J. Sens.*, 1-10.
- Cheon, D., Jung, Y., Park, E., Song, W. and Jang, H. (2011), "Evaluation of damage level for rock slopes using acoustic emission technique with waveguides", *Eng. Geol.*, **121**(1), 75-88.
- Committee on Fracture Characterization and Fluid Flow (1996), *Rock Fractures and Fluid Flow: Contemporary Understanding and Applications*, National Academic Press, Washington, U.S.A.
- Dyskin, A.V. (2003), "Influence of shape and locations of initial 3-D cracks on their growth in uniaxial compression", *Eng. Fract. Mech.*, **70**(15), 2115-2136.
- Deng, Q. and Zhang, P. (1984), "Research on the geometry of shear fracture zones", *J. Geophys. Res.*, **89**(B7), 5669-5710.
- Dey, T.N. and Wang, C.Y. (1981), "Some mechanisms of microcrack growth and interaction in compressive rock failure", *J. Rock Mech. Min. Sci. Geomech. Abstr.*, **18**(3), 199-209.
- Einstein, H.H., Veneziano, D., Baecher, G.B. and O'Reilly, K.J. (1983), "The effect of discontinuity persistence on rock slope stability", *J. Rock Mech. Min. Sci. Geomech. Abstr.*, **20**(5), 227-236.
- Fredrich, J.T., Evans, B. and Wong, T.F. (1990), "Effect of grain size on brittle and semi brittle strength: Implications for micromechanical modelling of failure in compression", *J. Geophys. Res.*, **95**(B7), 10907-10920.
- Gehle, C. and Kutter, H.K. (2003), "Breakage and shear behavior of intermittent rock joints", *J. Rock Mech. Min. Sci.*, **40**(5), 687-700.
- Germanovich, L.N., Carter, B.J., Dyskin, A.V., Ingraffea, A.R. and Lee, K.K. (1996), "Mechanics of 3-D crack growth under compressive loads", *Proceedings of the 2nd North American Rock Mechanics Symposium on Rock Mechanics Tools and Techniques*, Montreal, Canada, June.
- Germanovich, L.N., Salganik, R.L., Dyskin, A.V. and Lee, K.K. (1994), "Mechanisms of brittle fracture of rock with multiple pre-existing cracks in compression", *Pure Appl. Geophys.*, **143**(1), 17-149.
- Germanovich, L.N., Ring, L.M., Carter, B.J., Ingraffea, A.R., Dyskin, A.V. and Ustinov, K.B. (1995), "Simulation of crack growth and interaction in compression", *Proceedings of the 8th International Congress on Rock Mechanics*, Tokyo, Japan, September.
- Ghazvinian, A., Nikudel, M.R. and Sarfarazi, V. (2007), "Effect of rock bridge continuity and area on shear behavior of joints", *Proceedings of the 11th Congress of the International Society of Rock Mechanics*, Lisbon, Portugal, July.
- Griffith, A.A. (1921), "The phenomena of rupture and flow in solids", *Philos. Trans. R. Soc. London Ser. A.*, **221**, 163-198.
- Griffith, A.A. (1924), "The theory of rupture", *Proceedings of the 1st International Congress on Applied Mechanics*, Delft, The Netherlands, April.
- Haeri, H. (2015a), "Propagation mechanism of neighboring cracks in rock-like cylindrical specimens under uniaxial compression", *J. Min. Sci.*, **51**(3), 487-496.
- Haeri, H. (2015b), "Simulating the crack propagation mechanism of pre-cracked concrete specimens under shear loading conditions", *Strength Mater.*, **47**(4), 618-632.
- Haeri, H., Shahriar, K., Marji, M.F. and Moarefvand, P. (2014a), "On the cracks coalescence mechanism and cracks propagation paths in rock-like specimens containing pre-existing random cracks under compression", *J. Centr. South Univ.*, **21**(6), 2404-2414.
- Haeri, H., Shahriar, K., Marji, M.F. and Moarefvand, P. (2014b), "Investigating the fracturing process of rock-like Brazilian discs containing three parallel cracks under compressive line loading", *Strength Mater.*, **46**(3), 133-148.
- Haeri, H., Shahriar, K., Marji, M.F. and Moarefvand, P. (2015a), "On the HDD analysis of micro cracks initiation, propagation and coalescence in brittle substances", *Arab. J. Geosci.*, **8**(5), 2841-2852.
- Haeri, H., Marji, M.F. and Shahriar, K. (2015b), "Simulating the effect of disc erosion in TBM disc cutters by a semi-infinite DDM", *Arab. J. Geosci.*, **8**(6), 3915-3927.

- Haeri, H., Khaloo, A. and Marji, M.F. (2015c), "Experimental and numerical simulation of the microcracks coalescence mechanism in rock-like materials", *Strength Mater.*, **47**(1), 740-754.
- Haeri, H., Khaloo, A. and Marji, M.F. (2015d), "Experimental and numerical analysis of Brazilian discs with multiple parallel cracks", *Arab. J. Geosci.*, **8**(8), 5897-5908.
- Haeri, H. and Sarfarazi, V. (2016a), "The deformable multilaminar for predicting the elasto-plastic behavior of rocks", *Comput. Concrete*, **18**(2), 201-214.
- Haeri, H. and Sarfarazi, V. (2016b), "Numerical simulation of tensile failure of concrete using particle flow code (PFC)", *Comput. Concrete*, **18**(1), 39-51.
- Hall, S., De Sanctis, F. and Viggiani, G. (2006), "Monitoring fracture propagation in a soft rock (neapolitan tuff) using acoustic emissions and digital images", *Pure Appl. Geophys.*, **163**(10), 2171-2204.
- Hallbauer, D.K., Wagner, H. and Cook, N.G.W. (1973), "Some observations concerning the microscopic and mechanical behaviour of quartzite specimens in triaxial compression tests", *J. Rock Mech. Min. Sci. Geomech. Abstr.*, **10**(6), 713-726.
- Hoek, E. and Bieniawski, Z.T. (1984), "Brittle fracture propagation in rock under compression", *J. Fract.*, **26**(4), 276-294.
- Horii, H. and Nemat-Nasser, S. (1985), "Compression-induced microcrack growth in brittle solids: Axial splitting and shear failure", *J. Geophys. Res.*, **90**(B4), 3105-3125.
- Horii, S. and Nemat-Nasser, S. (1986), "Brittle failure in compression: splitting, faulting and brittle-ductile transition", *Phil. Trans. R. Soc. Lond. A*, **319**(1549), 337-374.
- Hu, B., Zhang, N. and Liu, S. (2009), "Contrastive model test for joint influence on strength and deformation of rock masses", *J. Centr. South Univ.*, **40**, 1133-1138.
- Huang, M.L., Tang, C.A. and Zhu, W.C. (1999), "Real-time SEM study on rock failure instability under uniaxial compression", *J. North Univ.*, **20**, 426-429.
- Hussain, M.A., Pu, E.L. and Underwood, J.H. (1974), "Strain energy release rate for a crack under combined mode I and mode II", *ASTM STP 1974*; **560**, 2-28.
- Ingraffea, A.R. and Heuze, F.E. (1980), "Finite element models for rock fracture mechanics", *J. Numer. Anal. Meth. Geomech.*, **4**(1), 25-43.
- Gerges, N., Issa, C. and Fawaz, S. (2015), "Effect of construction joints on the splitting tensile strength of concrete", *Case Stud. Constr. Mater.*, **3**, 83-91.
- Irwin, G.R. (1957), "Analysis of stresses and strains near the ends of a crack traversing a plate", *J. Appl. Mech.*, **24**(3), 361-364.
- Jaeger, J.C. (1971), "Friction of rocks and stability of rock slopes", *Geotech.*, **21**(2), 97-134.
- Jamil, S.M. (1999), "Strength of non-persistent rock joints", Ph.D. Dissertation, University of Illinois at Urbana-Champaign, Illinois, U.S.A.
- Jansen, D.P., Carlson, S.R., Young, R.P. and Hutchins, D.A. (1993), "Ultrasonic imaging and acoustic emission monitoring of thermally induced microcracks in Lac du Bonnet granite", *J. Geophys. Res.*, **98**(B12), 22231-22243.
- Jennings, J.E. (1970), "A mathematical theory for the calculation of the stability of slopes in open cast mines", *Proceedings of the Symposium on the Theoretical Background to the Plannings of Open Pit Mines with Special Reference to Slope Stability*, Johannesburg, South Africa, August.
- Jiefan, H., Ganglin, C., Yonghong, Z. and Ren, W. (1990), "An experimental study of the strain field development prior to failure of a marble plate under compression", *Tectonophys.*, **175**(6), 269-284.
- Kemeny, J.M. (1991), "A model for non-linear rock deformation under compression due to subcritical crack growth", *J. Rock Mech. Min. Sci. Geomech. Abstr.*, **28**(3), 459-467.
- Kemeny, J.M. and Cook, N.G.W. (1987), "Crack models for the failure of rock under compression", *Proceedings of the 2nd International Conference on Constitutive Laws for Engineering Materials*, Tucson, Arizona, U.S.A., January.
- Kim, J. and Taha, M.R. (2014), "Experimental and numerical evaluation of direct tension test for cylindrical concrete specimens", *Adv. Civil Eng.*, 1-8.
- Kim, W.J., Lee, J.M., Kim, J.S. and Lee, C.J. (2012), "Measuring high speed crack propagation in concrete fracture test using mechanoluminescent material", *Smart Struct. Syst.*, **10**(6), 547-555.

- Kranz, R.L. (1979), "Crack-crack and crack-pore interactions in stressed granite", *J. Rock Mech. Min. Sci. Geomech. Abstr.*, **16**(1), 37-47.
- Kranz, R.L. (1983), "Microcracks in rocks: A review", *Tectonophys.*, **100**(1-3), 449-480.
- Kumar, S. and Barai, S.V. (2012), "Size-effect of fracture parameters for crack propagation in concrete: A comparative study", *Comput. Concrete*, **9**(1), 1-19.
- Kuntz, M. and Lavallee, P. (1998), "Steady-state flow experiments to visualise the stress field and potential crack trajectories in 2D elastic-brittle cracked media in uniaxial compression", *J. Fract.*, **92**(4), 349-357.
- Lajtai, E.Z. (1969a), "Strength of discontinuous rocks in direct shear", *Geotech.*, **19**(2), 218-332.
- Lajtai, E.Z. (1969b), "Shear strength of weakness planes in rock", *J. Rock Mech. Min. Sci.*, **6**(5), 499-515.
- Lee, H. and Jeon, S. (2011), "An experimental and numerical study of fracture coalescence in pre-cracked specimens under uniaxial compression", *J. Sol. Struct.*, **48**(6), 979-999.
- Li, Y.P. and Wang, Y.H. (2003), "Analysis on zigzag cracks in rock-like materials under compression", *Acta Mech. Sol. Sinic.*, **24**(4), 456-462.
- Li, Y., Chen, L. and Wang, Y. (2005), "Experimental research on pre-cracked marble under compression", *J. Sol. Struct.*, **42**(9), 2505-2516.
- Lin, P., Zhou, W.Y. and Liu, H.Y. (2014), "Experimental study on cracking, reinforcement and overall stability of the xiaowan super-high arch dam", *Rock Mech. Rock Eng.*, **48**(2), 819-841.
- Liu, H.Y., Kou, S.Q., Lindqvist, P.A. and Tang, C.A. (2004), "Numerical simulation of shear fracture (mode II) in heterogeneous brittle rock", *J. Rock Mech. Min. Sci.*, **41**, 14-19.
- Mao, H. and Yang, C. (2009), "Analysis of deformation features of slates with structural surfaces", *Chin. J. Undergr. Space Eng.*, **2009**(5), 934-938.
- Mughieda, O. and Alzoubi, A.K. (2001), "Fracture mechanisms of open offset rock joints under uniaxial loading", M.S. Dissertation, Jordan University of Science and Technology, Irbid, Jordan.
- Mughieda, O. and Alzoubi, A. (2004), "Fracture mechanisms of offset rock joints-a laboratory investigation", *Geotech. Geol. Eng.*, **22**(4), 545-562.
- Mughieda, O. and Karasneh, I. (2006), "Coalescence of offset rock joints under biaxial loading", *Geotech. Geol. Eng.*, **24**(4), 985-999.
- Nemat-Nasser, S. and Horii, H. (1982), "Compression-induced non-planar crack extension with application to splitting, exfoliation and rockburst", *J. Geophys. Res.*, **87**(B8), 6805-6821.
- Ning, J., Liu, X., Tan, Y., Wang, J. and Tian, C. (2015), "Relationship of box counting of fractured rock mass with Hoek-Brown parameters using particle flow simulation", *Geomech. Eng.*, **9**, 619-629.
- Olsson, W.A. and Pang, S.S. (1976), "Microcrack nucleation in marble", *J. Rock Mech. Min. Sci. Geomech. Abstr.*, **13**(2), 53-59.
- Panaghi, K., Golshani, A. and Takemura, T. (2015), "Rock failure assessment based on crack density and anisotropy index variations during triaxial loading tests", *Geomech. Eng.*, **9**, 793-813.
- Pang, S. and Jonson, A.M. (1972), "Crack growth and faulting in cylindrical specimens of chelmsford granite", *J. Rock Mech. Min. Sci. Geomech. Abstr.*, **9**(1), 37-86.
- Papadopoulos, G.A. and Poniridis, P.I. (1989), "Crack initiation under biaxial loading with higher-order approximation", *Eng. Fract. Mech.*, **32**(3), 351-360.
- Park, N.S. and Jeon, S.W. (2001), "The crack coalescence in rock bridges under uniaxial compression", **3**(2), 23-32.
- Petit, J. and Barquins, M. (1988), "Can natural faults propagate under mode II conditions?" *Tecton.*, **7**(6), 1243-1256.
- Prudencio, M. and Van Sint Jan, M. (2007), "Strength and failure modes of rock mass models with non-persistent joints", *J. Rock Mech. Min. Sci.*, **44**(6), 890-902.
- Pu, C., Cao, P. and Zhao, Y. (2010), "Numerical analysis and strength experiment of rock-like materials with multi-fissures under uniaxial compression", *Rock Soil Mech.*, **31**(11), 3661-3666.
- Reyes, O. (1991), "Experimental study, analytic modeling of compressive fracture in brittle materials", Ph.D. Dissertation, Massachusetts Institute of Technology, Cambridge, U.S.A.
- Rudajev, V., Číž, R., Lokajíček, T. and Vilhelm, J. (2000), "Geological structure, seismic energy release and forecasting of rockburst occurrence", *Acta Montan. Ser. A*, **16**(118), 171-174.

- Sagong, M. and Bobet, A. (2000), "Coalescence of multiple flaws in uniaxial compression", *Proceedings of the North American Rock Mechanics Symposium: Pacific Rocks*, Seattle, Washington, U.S.A., July.
- Sagong, M. and Bobet, A. (2002), "Coalescence of multiple flaws in a rock-model material in uniaxial compression", *J. Rock Mech. Min. Sci.*, **39**, 229-241.
- Sahouryeh, E. (2002), "Crack growth under biaxial compression", *Eng. Fract. Mech.*, **69**, 2187-2198.
- Sammis, C.G. and Ashby, M.F. (1986), "The failure of brittle porous solids under compressive stress states", *Acta Metall.*, **34**(3), 511-526.
- Sardemir, M. (2016), "Empirical modeling of flexural and splitting tensile strengths of concrete containing fly ash by GEP", *Comput. Concrete*, **17**(4), 489-498.
- Sarfrazi, V. and Haeri, H. (2016), "The effect of non-persistent joints on sliding direction of rock slopes", *Comput. Concrete*, **17**, 723-737.
- Sarfrazi, V., Faridi, H.R., Haeri, H. and Schubert, W. (2015), "A new approach for measurement of anisotropic tensile strength of concrete", *Adv. Concrete Constr.*, **3**(4), 269-284.
- Savilahti, T., Nordlund, E. and Stephansson, O. (1990), "Shear box testing and modeling of joint bridge", *Proceedings of the International Symposium on Shear Box Testing and Modeling of Joint Bridge Rock Joints*, Loen, Norway, June.
- Shah, S.P. (1999a), "Fracture toughness for high-strength concrete", *ACI Mater.*, **87**(3), 260-265.
- Shah, S.P. (1999b), "Experimental methods for determining fracture process zone and fracture parameters", *Eng. Fract. Mech.*, **35**, 3-14.
- Shang, J.L., Kong, C.J., Li, T.J. and Zhang, W.Y. (1999), "Observation and study on meso-damage and fracture of rock", *J. Exp. Mech.*, **14**(3), 373-383.
- Shen, B. (1993), "The mechanics of fracture coalescence in compression experimental study and numerical simulation", *Eng. Fract. Mech.*, **51**(1), 73-85.
- Shen, B., Stephansson, O., Einstein, H.H. and Ghahreman, B. (1995), "Coalescence of fracture under shear stresses in experiments", *J. Geophys. Res.*, **100**(B4), 725-729.
- Steif, P.S. (1984), "Crack extension under compressive loading", *Eng. Fract. Mech.*, **20**(3), 463-473.
- Stimpson, B. (1978), "Failure of slopes containing discontinuous planar joints", *Proceedings of the 19th US Symposium on Rock Mechanics*, Reno, U.S.A., May.
- Takeuchi, K. (1991), "Mixed-mode fracture initiation in granular brittle materials", M.S. Dissertation, Massachusetts Institute of Technology, Cambridge, U.S.A.
- Tang, C.A. and Kou, S.Q. (1998), "Fracture propagation and coalescence in brittle materials", *Eng. Fract. Mech.*, **61**(3), 311-324.
- Tang, C.A. (1997), "Numerical simulation of progressive rock failure and associated seismicity", *J. Rock Mech. Min. Sci.*, **34**(2), 249-262.
- Tang, H.D., Zhu, Z.D., Zhu, M.L. and Lin, H.X. (2015), "Mechanical behavior of 3D crack growth in transparent rock-like material containing preexisting flaws under compression", *Adv. Mater. Sci. Eng.*, 1-10.
- Tapponnier, P. and Brace, W.F. (1976), "Development of stress-induced micro-cracks in westerly granite", *J. Rock Mech. Min. Sci. Geomech. Abstr.*, **13**(4), 103-112.
- Wen, W. (2013), "Experimental study on rock-like material with pre-cracks under uniaxial compression", *EJGE*, **18**, 1775-1785.
- Weihua, Z., Runqiu, H. and Ming, Y. (2015), "Mechanical and fracture behavior of rock mass with parallel concentrated joints with different dip angle and number based on PFC simulation", *Geomech. Eng.*, **8**(6), 757-767.
- Wong, R.H.C. and Chau, K.T. (1998), "Crack coalescence in a rock-like material containing two cracks", *J. Rock Mech. Min. Sci.*, **35**(2), 147-164.
- Wong, R.H.C. and Chau, K.T. (1997), "The coalescence of frictional cracks and the shear zone formation in brittle solids under compressive stresses", *J. Rock Mech. Min. Sci.*, **34**(3/4), 366.
- Wong, R.H.C. and Chau, K.T. (1998), "Peak strength of replicated and real rocks containing cracks", *Key Eng. Mater.*, **145**, 953-958.
- Wong, R.H.C., Chau, K.T., Tang, C.A. and Lin, P. (2001), "Analysis of crack coalescence in rock-like

- materials containing three flaws-part I: Experimental approach”, *J. Rock Mech. Min. Sci.*, **38**(7), 909-924.
- Wong, R.H.C., Lin, P., Tang, C.A. and Chau, K.T. (2002), “Creeping damage around an opening in rock-like material containing non-persistent joints”, *Eng. Fract. Mech.*, **69**(17), 2015-2027.
- Yin, L. and Zhang, P. (2010), “Simulation analysis of rock mass strength affected by dual structural plane”, *J. Min. Safety Eng.*, **2010**(27), 600-603.
- Yang, S.Q. (2015), “An experimental study on fracture coalescence characteristics of brittle sandstone specimens combined various flaws”, *Geomech. Eng.*, **8**(4), 541-557.
- Xiang, F., Kulailake, P.H.S.W., Xin, C. and Ping, C. (2015), “Crack initiation stress and strain of jointed rock containing multi-cracks under uniaxial compressive loading: A particle flow code approach”, *J. Centr. South Univ.*, **22**(2), 638-645.
- Zhang, X. and Wong, L.N.Y. (2012), “Cracking process in rock-like material containing a single flaw under uniaxial compression: A numerical study based on parallel bonded-particle model approach”, *Rock Mech. Rock Eng.*, **45**(5), 711-737.
- Zhang, X. and Wong, R.H.C. (2013), “Crack initiation, propagation and coalescence in rock-like material containing two flaws: A numerical study based on bonded-particle model approach”, *Rock Mech. Rock Eng.*, **46**(5), 1001-1021.
- Zhang, X.P. and Wong, L.N.Y. (2012), “Cracking process in rock-like material containing a single flaw under uniaxial compression: A numerical study based on parallel bonded-particle model approach”, *Rock Mech. Rock Eng.*, **45**(5), 711-737.
- Zhao, Y.H., Liang, H.H., Huang, J.F., Geng, J.D. and Wang, R. (1995), “Development of sub cracks between en echelon fractures in rock plates”, *Pure Appl. Geophys.*, **145**, 759-773.
- Zhao, C. (2015), “Analytical solutions for crack initiation on floor-strata interface during mining”, *Geomech. Eng.*, **8**(2), 237-255.
- Zhu, W.S., Chen, W.Z. and Shen, J. (1998), “Simulation experiment and fracture mechanism study on propagation of Echelon pattern cracks”, *Acta Mech. Sol. Sinic.*, **19**, 355-360.